

This is a repository copy of *Holocene mangrove dynamics and relative sea-level changes along the Tanzanian coast, East Africa*.

White Rose Research Online URL for this paper:

<https://eprints.whiterose.ac.uk/136117/>

Version: Accepted Version

Article:

Punwong, Paramita, Selby, Katherine Anne orcid.org/0000-0002-3055-2872 and Marchant, Robert orcid.org/0000-0001-5013-4056 (2018) Holocene mangrove dynamics and relative sea-level changes along the Tanzanian coast, East Africa. *Estuarine coastal and shelf science*. pp. 105-117. ISSN 0272-7714

<https://doi.org/10.1016/j.ecss.2018.07.004>

Reuse

This article is distributed under the terms of the Creative Commons Attribution-NonCommercial-NoDerivs (CC BY-NC-ND) licence. This licence only allows you to download this work and share it with others as long as you credit the authors, but you can't change the article in any way or use it commercially. More information and the full terms of the licence here: <https://creativecommons.org/licenses/>

Takedown

If you consider content in White Rose Research Online to be in breach of UK law, please notify us by emailing eprints@whiterose.ac.uk including the URL of the record and the reason for the withdrawal request.

1
2
3
4 1 Holocene mangrove dynamics and relative sea-level changes along the Tanzanian
5
6 2 coast, East Africa

7
8 3 Paramita Punwong^{1, 2*}, Katherine Selby³, Rob Marchant²
9

10 4

11
12 5 ¹ Faculty of Environment and Resource Studies, Mahidol University, Nakhon
13
14 6 Pathom, 73170, Thailand

15
16 7 ² York Institute of Tropical Ecosystems, Environment Department, University of
17
18 8 York, York YO10 5NG, UK

19
20 9 ³ Environment Department, University of York, York YO10 5NG, UK
21
22

23 10

24
25 11 **Abstract** There is continued uncertainty regarding the rate, timing, duration and
26
27 12 direction of Holocene sea-level for the Indian Ocean, and indeed the wider
28
29 13 tropical realm. We present the first synthesis, and a new chronology, for
30
31 14 Holocene relative sea-level (RSL) using a range sediment cores retrieved from
32
33 15 mangrove ecosystems in three locations along coastal Tanzania. This study
34
35 16 applies the relationship of ratios between the key mangrove taxa of
36
37 17 *Sonneratia:(Bruguiera/Ceriops)* (S/BC) (ranging from 0 – 22.9) and
38
39 18 *Sonneratia:Rhizophora* (S/R) (ranging from 0 – 2.29), vegetation and altitude to
40
41 19 interpret mangrove dynamics and refine the vertical errors associated with relative
42
43 20 sea level change. The variations in mangrove taxa ratios in the sediment cores
44
45 21 obtained from each site shows mangrove development at different periods during
46
47 22 the Holocene from around 7900 cal yr BP. An early to mid-Holocene RSL rise
48
49 23 occurred from ~7900 to ~4600 cal yr BP that may have reached a higher level
50
51 24 than present. A lower RSL occurred after 4600 cal yr BP, resulting in mangroves
52
53 25 retreating seaward at all three study locations, before a low magnitude RSL rise
54
55
56
57
58
59
60

61
62
63
64 26 occurred between 4400 and 2000 cal yr BP. Another RSL rise is recorded at ~
65
66 27 500 cal yr BP before falling to a level lower than present at ~100 cal yr BP. There
67
68 28 is evidence of a recent RSL rise recorded from mangrove ratios during the last
69
70 29 century. In addition, the sedimentation rates among sites are relatively different
71
72 30 due to different altitudinal ranges with freshwater input, sediment supply and
73
74 31 progradation having significantly more effect in the Rufiji Delta (2.1-10.9 mm cal
75
76 32 yr⁻¹) than at the Zanzibar sites (0.3-6.6 mm cal yr⁻¹).
77
78
79 33

80
81 34 Keywords: Indian Ocean, pollen-vegetation relationships, far-field locations,
82
83 35 Zanzibar, Rufiji Delta
84

85 36

86
87 37 *Corresponding author.
88

89 38 E-mail: punnbio@gmail.com; paramita@mahidol.edu
90
91
92
93
94
95
96
97
98
99
100
101
102
103
104
105
106
107
108
109
110
111
112
113
114
115
116
117
118
119
120

121
122
123
124 39 1. Introduction
125

126 40 Relative sea-level (RSL) (the height of the ocean with respect to the
127
128 41 surface of the solid Earth) has fluctuated over time that has resulted in
129
130 42 geophysical and ecological changes (Pirazzoli, 1991). Far-field sites, located at a
131
132 43 distance from the major ice sheets, are important locations for reconstructing RSL
133
134 44 changes. Far-field locations can provide important constraints on global RSL
135
136 45 change when combined with more intensively studied temperate areas, where
137
138 46 coastal adjustments following removal of ice loading are most acute, especially
139
140
141 47 during the mid and late Holocene (Milne and Mitrovica, 2008).
142

143 48 Holocene RSL changes in far-field locations result from eustatic changes,
144
145 49 equatorial syphoning and hydro-isostasy (continental levering) (Mitrovica and
146
147 50 Milne, 2002; Milne and Mitrovica, 2008). Equatorial ocean syphoning results
148
149 51 from collapsing forebulges at the near-field continental margins that cause RSL
150
151 52 fall to be recorded in far-field locations (Mitrovica and Peltier, 1991). Continental
152
153 53 levering occurs when there is water loading due to deglaciation, that causes
154
155 54 continental subsidence and an uplift of the adjacent continents, inducing RSL fall
156
157
158 55 at areas distant from the continental margins (Lambeck and Nakada, 1990;
159
160 56 Mitrovica and Milne, 2002; Gehrels and Long, 2008). RSL records from far-field
161
162 57 locations have been produced from various locations including the Indian Ocean
163
164 58 (Katupotha and Fujiwara, 1988; Banjeree, 2000), Southeast Asia (Hanebuth et al.,
165
166 59 2000; Horton et al., 2005; Bird et al., 2007) and Australia (Lambeck and Nakada,
167
168 60 1990; Larcombe et al., 1995; Lewis et al., 2013). Holocene RSL changes have
169
170 61 been reconstructed from Australia using a range of coastal and coral reef proxies;
171
172 62 some studies suggest a highstand at ~6000 cal yr BP (Lambeck and Nakada, 1990;
173
174 63 Larcombe et al., 1995), whereas others indicate a later highstand around 3900 cal
175
176
177
178
179
180

181
182
183
184 64 yr BP (Baker et al., 2001). A review of geo-chronological data from along the
185
186 65 southeast coast of Australia, indicates a highstand from 7700 cal yr BP that lasted
187
188 66 until about 2000 cal yr BP, before falling to the present-day level (Sloss et al.,
189
190 67 2007). In the northern Indian Ocean, two mid-late Holocene highstands, one at
191
192 68 7300 cal yr BP and another at 4300 cal yr BP, have been recorded from beach
193
194 69 ridges and coral terraces along the east coast of India (Banerjee, 2000). These
195
196 70 highstands were also recorded from corals and marine shells along the southwest
197
198 71 and south coasts of Sri Lanka (Katupotha and Fujiwara, 1988) occurring at 6500
199
200
201 72 cal yr BP and 3200 cal yr BP.

202
203 73 Clearly far-field RSL records are of immense value for understanding and
204
205 74 constraining sea level records but there is a range of timings and duration of these.
206
207 75 In this paper we present evidence of RSL changes derived from three mangrove
208
209 76 sediment records (Punwong et al., 2012; 2013a; 2013b) from sites on the
210
211 77 Tanzanian coast. Combined, these data provide the first sea-level curve and a
212
213 78 refined chronology for Holocene RSL and coastal changes for Tanzania. This
214
215 79 study also uses the relationship between ratios of key mangrove taxa, vegetation
216
217 80 and altitude to interpret mangrove dynamics and refine the vertical errors of RSL
218
219 81 change. Holocene RSL changes are integrated with existing RSL reconstructions
220
221 82 from the region to develop a reconstruction of Holocene RSL changes across the
222
223 83 Southwest Indian Ocean.

224
225
226 84

227 228 85 1.1. Sea-level history in the southwest Indian Ocean

229
230 86 The record of Holocene RSL change along the East African coast, situated
231
232 87 in the tectonically stable (Woodroffe and Horton, 2005) Southwest Indian Ocean,
233
234 88 is poorly constrained (Pirazzoli, 1991; Camoin et al., 2004). Reconstructed RSL
235
236
237
238
239
240

241
242
243
244 89 changes are available from only a few locations and use a range of different
245
246 90 proxies (Figure 1a). Previous studies of RSL change on the continental coasts of
247
248 91 east and southeast Africa (Mozambique and South Africa) indicate that RSL rose
249
250 92 rapidly during the early Holocene and reached the present level by the mid
251
252 93 Holocene (Jaritz et al., 1977, Ramsay, 1995; Ramsay and Cooper, 2002; Norström
253
254 94 et al., 2012). Mid Holocene highstands of up to 3.5 m above the present level
255
256 95 were recorded by 5000 cal yr BP, followed by subsequent falls to the present level
257
258 96 in the late Holocene. A different RSL reconstruction derived from coral from the
259
260 97 offshore islands (Mauritius, Mayotte and Réunion Island) shows that a rapid RSL
261
262 98 rise occurred during the early Holocene reaching present level at ~3000 cal yr BP
263
264 99 with no evidence for a mid Holocene highstand (Camoin et al., 1997; 2004;
265
266 100 Colonna et al., 1997; Zinke et al., 2003). Although all RSL studies within this
267
268 101 region record an early Holocene RSL rise, there is considerable uncertainty on the
269
270 102 amplitude and timing of this. The varied environmental settings and distances
271
272 103 from formerly glaciated areas would result in different isostatic contributions to
273
274 104 RSL changes. For example, it is thought that small offshore volcanic islands are
275
276 105 less affected by hydro-isostatic adjustment than those studies from continental
277
278 106 locations due to the effects of continental levering during the mid and late
279
280 107 Holocene (Camoin et al., 2004; Lambeck and Nakada, 1990; Mitrovica and
281
282 108 Milne, 2002; Milne and Mitrovica, 2008). The different proxies used make it
283
284 109 likely that the sea-level index points may not be comparable and some sea-level
285
286 110 index points may have large indicative ranges and different degrees of precision
287
288 111 (Jaritz et al., 1977; Ramsay, 1995; Ramsay and Cooper, 2002; Woodroffe and
289
290 112 Horton, 2005; Norström et al., 2012).

291
292
293
294
295 113
296
297
298
299
300

301
302
303
304 114 1.2. Mangrove as sea-level indicators
305

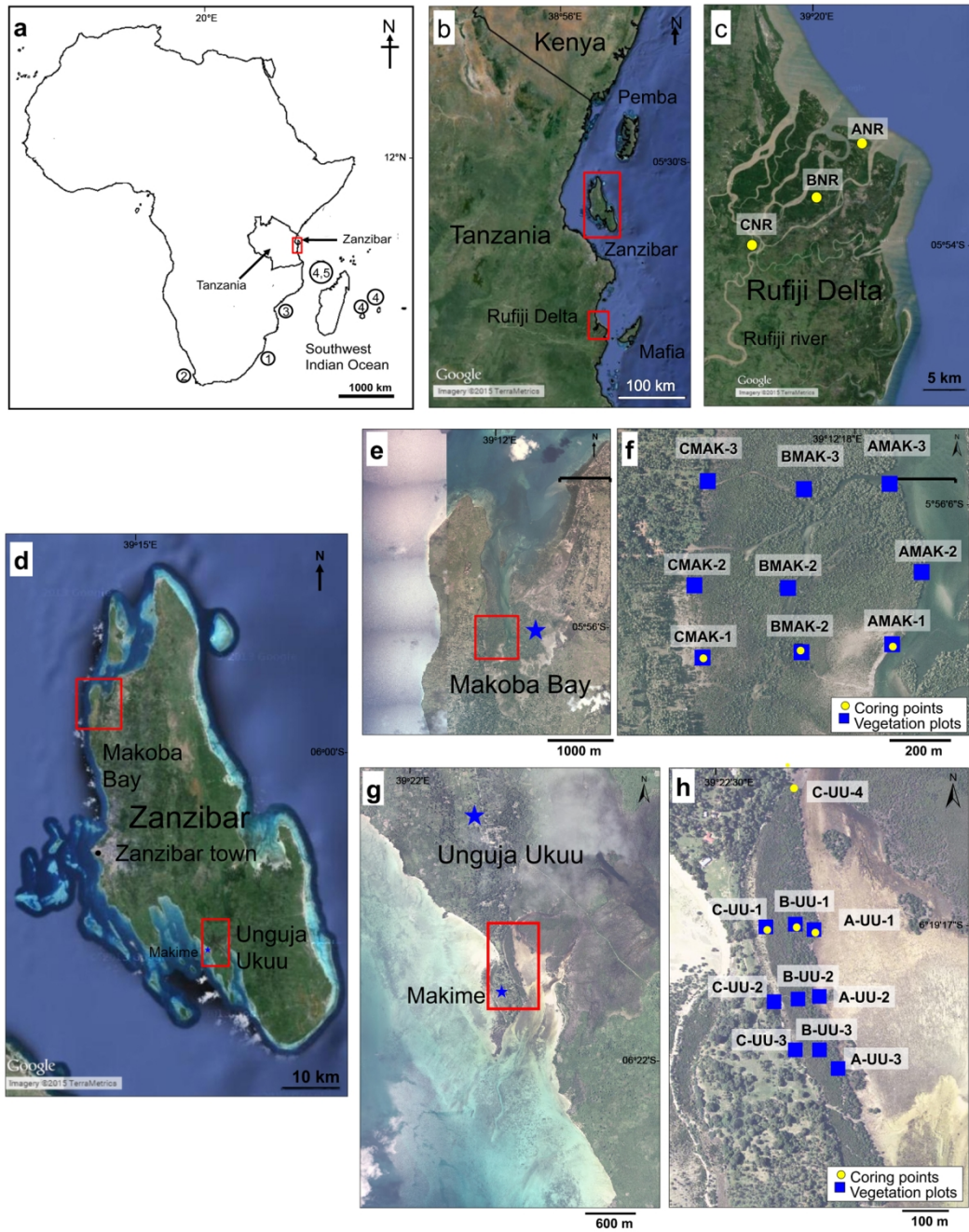
306 115 Research on RSL reconstruction from far-field locations has traditionally
307
308 116 focused on coring and dating corals (Pirazzoli, 1988; Fairbanks, 1989; Colonna et
309
310 117 al., 1997; Camoin et al., 1997, 2004). However, sediments that accumulate within
311
312 118 mangrove ecosystems can also be used to reconstruct RSL and coastal changes.
313
314 119 Mangrove ecosystems are found in coastal tropical regions along the margins of
315
316 120 the sea and lagoons; they are characterised by evergreen trees and shrubs that are
317
318 121 physiologically and morphologically adapted to grow in the sub-tropical to
319
320 122 tropical intertidal zone between mean sea level and the high water of spring tide
321
322 123 (Woodroffe and Grindrod, 1991; Blasco et al., 1996; Ellison and Farnsworth,
323
324 124 2001; Ellison, 2008). Mangrove ecosystems respond to changes in sea level by
325
326 125 migrating landwards with a rise in sea level or seawards with a fall (Gilman et al.,
327
328 126 2008). Mangrove community composition is able to keep pace with sea-level
329
330 127 changes (McIvor et al., 2013). For mangroves to be able to withstand sea level
331
332 128 rise, the rates of sedimentary accretion within the mangrove has to be equivalent
333
334 129 to the rate of sea-level rise (Ellison, 2015), otherwise mangroves may undergo *in*
335
336 130 *situ* drowning leading to weakened root structures, dieback and disappearance
337
338 131 (Gilman et al., 2008).
339
340
341

342 132 Santisuk (1983) and Watson (1928) classified mangroves into a series of
343
344 133 inundation class zones according to ecological preference to monthly inundation
345
346 134 frequency. *Rhizophora mucronata*, *Avicennia marina*, *Sonneratia alba*, *Bruguiera*
347
348 135 *gymnorhiza* and *Ceriops tegal* are classified as true mangroves or mangroves.
349
350 136 The term true mangroves are also defined as mangroves representing trees and
351
352 137 shrubs growing in the areas inundated by the normal to all high tides. Back
353
354 138 mangroves such as *Heritiera littoralis* and *Acrostichum aureum* are plants
355
356
357
358
359
360

361
362
363
364 139 growing in the areas inundated by the sea only during spring high tides,
365
366 140 exceptional high tides, or during cyclones. The dominance of mangrove species
367
368 141 which occurs in zones throughout the mangrove ecosystem can thus be an
369
370 142 indicator of sea-level fluctuations by comparing the relationships between
371
372 143 contemporary vegetation assemblages and their inundation frequency with respect
373
374 144 to sea level.

375
376 145 Mangrove pollen has previously been used to reconstruct compositional
377
378 146 changes in mangrove ecosystems (e.g. Cohen et al., 2005; Horton et al., 2005;
379
380 147 Vedel et al., 2006; Tossou et al., 2008; Hait and Behling, 2009) including in East
381
382 148 Africa (Punwong et al., 2012; 2013a; 2013b). Engelhart et al. (2007) developed a
383
384 149 transfer function from a modern analogue of mangrove surface pollen
385
386 150 assemblages that has been used to predict the palaeo mangrove elevation with
387
388 151 precision of ± 0.22 m. A contemporary study into the relationships between
389
390 152 mangrove pollen in surface sediment samples and the composition of the
391
392 153 vegetation indicated that majority of pollen was local in origin reflecting
393
394 154 vegetation in close proximity to the sampling sites (Punwong et al., 2013a,
395
396 155 2013b). Pollen accumulated in sediments underlying mangroves, in combination
397
398 156 with an understanding of the present relationship of mangrove composition to the
399
400 157 altitude of present sea level, can be used to reconstruct RSL fluctuations (Ellison,
401
402 158 1989; 2005; 2008; Punwong et al., 2012; 2013a; 2013b).
403
404
405
406
407
408
409
410
411
412
413
414
415
416
417
418
419
420

421
422
423
424
425
426
427
428
429
430
431
432
433
434
435
436
437
438
439
440
441
442
443
444
445
446
447
448
449
450
451
452
453
454
455
456
457
458
459
460
461
462
463
464
465
466
467
468
469
470
471
472
473
474
475
476
477
478
479
480



159

160 Figure 1. (a) Map of the Southwest Indian Ocean showing the location of
161 Tanzania and previous sea level studies: (1) Ramsay and Cooper (2002), (2)
162 Compton (2001), (3) Jaritz et al. (1977), (4) Colonna et al. (1996); Camoin et al.
163 (1997), (5) Zinke (2000); Zinke et al. (2003). (b) Map of the coast of Tanzania
164 showing the location of the Rufiji Delta (c) and Zanzibar (d). Inset e, f, g and h
165 show where the sedimentary cores were taken and the location of vegetation plots
166 located in Makoba Bay and Unguja Ukuu respectively.

481
482
483
484 167

485
486 168 2. Study sites

487
488 169

489
490 170 2.1. Geology and geomorphology

491
492 171 The three sites investigated are all characterised by mangrove forest and
493
494 172 located in the northern Rufiji Delta (Tanzanian mainland), Makoba Bay and
495
496 173 Unguja Ukuu (Unguja island, Zanzibar) (Figure 1b-h). The Rufiji Delta consists
497
498 174 of mangrove forest that grades into paddy fields at higher elevations and supports
499
500 175 the largest expanse of estuarine mangrove along the East African coast
501
502 176 (Nshubemuki, 1993; Fisher et al., 1994; Richmond et al., 2002; Masalu, 2003;
503
504 177 Mangora et al., 2016). The deltaic area is covered by fluvial sand, silt and clay
505
506 178 (Semesi, 1992) (Figure 1c). A series of sand spit islands and submerged sand bars
507
508 179 have formed parallel to the seaward margins (Fisher et al., 1994), while clayey
509
510 180 silts and silty clays containing organic matter characterise the mangrove
511
512 181 sediments. The average tidal range is 2 - 2.5 m and approximately 3.3 - 4.3 m on
513
514 182 high spring tides (Francis, 1992; Fisher et al., 1994; Richmond et al., 2002).

515
516
517 183 Unguja Island (Zanzibar) is located on the continental shelf some 40 km
518
519 184 from the mainland. The island has been periodically part of the mainland when
520
521 185 sea level was 30-40 m below present sea level and the last separation from the
522
523 186 mainland by sea-level inundation of the Zanzibar channel occurred at the end of
524
525 187 the Pleistocene to early Holocene (Prendergast et al., 2016). Most of Unguja
526
527 188 consists of Pleistocene reef limestone often outcropping on the east coast
528
529 189 (Shunula, 2002) with alluvial deposits locally present (Schlüter, 1997; Arthurton
530
531 190 et al., 1999) although there are no large rivers (Shunula, 2002). It is influenced by
532
533 191 a semi-diurnal tide, ranging from 2 m on neap tide to 4 m on spring tide
534
535
536
537
538
539
540

541
542
543
544 192 (Mwandya et al., 2010). The study areas are located in the northwest of Makoba
545
546 193 Bay (Figure 1d; 1e) and the east Makime headland of Unguja Ukuu (Figure 1d;
547
548 194 1g).

549
550 195

552 196 2.2. Climate

554 197 The rainfall pattern within the Rufiji Delta and on Zanzibar is largely
555
556 198 controlled by the north and south migration of the Inter-tropical Convergence
557
558 199 Zone (ITCZ). For the Rufiji delta, the northeast monsoon prevails from December
560
561 200 to April bringing heavy rainfall (Goudie, 1996; Nicholson, 2001) and the
562
563 201 southeast monsoon dominates from May to November bringing less rainfall
565
566 202 (Fisher et al., 1994; Richmond et al., 2002). The average annual rainfall is about
567
568 203 1200 mm yr⁻¹ (Semesi, 1992) and the temperature range throughout the year is 24
569
570 204 - 31 °C (Richmond et al., 2002). For Zanzibar, the northeast and southeast
571
572 205 monsoons bring the long rains from March to May and short rains from October
573
574 206 to December (Machiwa and Hallberg, 1995; Mwandya et al., 2010). The mean
575
576 207 annual rainfall is about 1500 -1800 mm yr⁻¹ (Knopp et al., 2008) and the average
577
578 208 temperature range throughout the year is about 27 - 30 °C (Machiwa and
579
580 209 Hallberg, 1995).

581
582 210

584 211 3. Methodology

585
586 212

588 213 3.1. Coring

590 214 Three sediment cores were retrieved from each site at a seaward, central and
591
592 215 landward location using a Russian corer along a transect perpendicular to the
593
594 216 coastline through the centre of mangrove forests to reduce the influence of local
595
596
597
598
599
600

601
602
603
604 217 land-based edge effects such as erosion or progradation from creeks (Ellison,
605
606 218 2008). The core depths varied between 1 to 4.5 m (Table 1) and each site was
607
608 219 cored until the sediment became impenetrable or bedrock was reached (Punwong
609
610 220 et al., 2012; 2013a; 2013b). The transect length varied depending on the nature of
611
612 221 the environmental setting and the extent of the mangrove area; this extended along
613
614 222 20 km in the northern Rufiji Delta (ANR, BNR, CNR), 600 m in Makoba Bay
615
616 223 (AMAK-1, BMAK-1, CMAK-1) and 80 m at Unguja Ukuu (A-UU-1, B-UU-1, C-
617
618 224 UU-1) (Figures 1c; 1f; 1h, Table 1). An additional sediment core was retrieved
619
620 225 from Unguja Ukuu (C-UU-4) at a location away from the transect as it represents
621
622 226 a longer sediment record than the other three cores.

625 227 3.2. Vegetation plots

627 228 To study the relationship between mangrove species composition, pollen
628
629 229 accumulating in the sediment and RSL, nine 20 m² vegetation plots were set up to
630
631 230 establish species percentages along an altitudinal gradient. At the three sites, there
632
633 231 was considerable variation in the horizontal distance covered to accommodate the
634
635 232 full range of the upper and the lower limits of mangroves. In the Rufiji Delta, the
636
637 233 vegetation survey transect along the large riverine mangrove system with
638
639 234 freshwater inputs covered 20 km. As the consequence, we were not able to carry
640
641 235 out adequate vegetation surveys and to set up plots within the restricted fieldwork
642
643 236 time frame. On Zanzibar the transects extended between 80 to 600 m of fringing
644
645 237 mangroves characterised by a similar composition across the three sites. Given
646
647 238 variations in the horizontal distance and vertical range, the mangrove gradient in
648
649 239 Zanzibar is considered to be steeper than the Rufiji Delta. A more detailed study
650
651 240 at both sites in Zanzibar allowed the ecosystem and structural composition at
652
653 241 different levels of sea-level inundation to be determined and inform the
654
655
656
657
658
659
660

661
662
663
664 242 reconstruction of past RSL fluctuations. Vegetation in nine 20 m² nested quadrats
665
666 243 was surveyed and recorded and surface sediment samples were collected (Figures
667
668 244 1f, 1h) from three seaward, three central and three landward sites, then considered
669
670 245 to be an upper intertidal, a middle intertidal and a lower intertidal mangrove
671
672 246 classes, respectively. Five cm³ of surface samples from the four corners and centre
673
674 247 of each plot were collected and subsequently used to study the relationship
675
676 248 between pollen presence and vegetation coverage. Altitudinal heights were
677
678 249 obtained using a differential GPS (dGPS model Leica TCRA total station and
679
680
681 250 Leica System 500 base and receiver with a manufacturer quoted vertical precision
682
683 251 of ± 0.001 m). Initial calibration of the dGPS occurred against recognised
684
685 252 National Datum benchmarks and subsequently all coring sites, vegetation plots
686
687 253 and full range of mangrove sites were levelled and calibrated to mean tide level
688
689 254 (MTL) (based on Admiralty Tide Tables, 2014). These altitudes were determined
690
691 255 relative to a benchmark at Kibiti for the Rufiji Delta using a known actual base
692
693 256 station Triangulation point (TTP 353) and the Ministry of Lands and the
694
695 257 Environment Benchmark (Zanzibar).

698 258

700 259 3.3. Palaeoecological analysis

702 260 The cores were sub-sampled every 10 cm and the volume of each subsample
703
704 261 was approximately 2 cm³ for pollen analysis (Punwong et al., 2012; 2013a;
705
706 262 2013b). The relationship between pollen assemblages and vegetation composition
707
708 263 was determined using three pollen association indices that reflect how accurately
709
710 264 pollen types reflect the abundance of their parent plant (Davis, 1984). The three
711
712 265 indices are ‘association index’ representing similar presence of the pollen and the
713
714 266 associated plant in the vegetation, ‘under-representation index’ representing

721
722
723
724 267 pollen percentages that are much lower than plant percentages, and ‘over-
725
726 268 representation index’ representing pollen percentages that exceed plant
727
728 269 percentages (Davis, 1984). Pearson’s Correlation Coefficients were used to
729
730 270 describe the relationship between pollen percentages extracted from the surface
731
732 271 sediment and plant percentages from the nine vegetation plots in Makoba Bay and
733
734 272 Unguja Ukuu.

736
737 273

738 274 3.4. Chronology

740
741 275 Twenty-six bulk sediment samples were selected for AMS dating and
742
743 276 submitted to the Radiocarbon Dating Laboratories at the University of Waikato,
744
745 277 New Zealand and the CHRONO Centre, Queen’s University Belfast, UK. At the
746
747 278 start of the laboratory work, dates were obtained from the base of the core with
748
749 279 targeted dating from different stratigraphic boundaries and key biostratigraphical
750
751 280 horizons occurring as the research developed. Additionally, nine dates from
752
753 281 AMAK-1 and BMAK-1 cores were obtained on organic concentrate samples
754
755 282 following Woodroffe et al. (2015a). Each 1 cm³ bulk sediment was deflocculated
756
757 283 using Na₄P₂O₄/ NaOH, heated with 10% HCl and sieved through a 10, 63 and 90
758
759 284 µm mesh. The 10-63 µm sieving fraction was selected for dating as it contained
760
761 285 fine organic material and pollen (Woodroffe et al., 2015a). The organic
762
763 286 concentrate samples were submitted for dating to the Natural Environment
764
765 287 Research Council (NERC) Radiocarbon Facility (East Kilbride) for AMS dating
766
767 288 (NERC Radiocarbon Facility Allocation 1608.0312). All dates were calibrated
768
769 289 using the southern hemisphere calibration Shcal04 curve (McCormac et al., 2004)
770
771 290 using the software OxCal v4.10 (Bronk-Ramsey, 2009).
772
773 291

774
775 291

721
722
723
724
725
726
727
728
729
730
731
732
733
734
735
736
737
738
739
740
741
742
743
744
745
746
747
748
749
750
751
752
753
754
755
756
757
758
759
760
761
762
763
764
765
766
767
768
769
770
771
772
773
774
775
776
777
778
779
780

781
782
783
784 292 4. Results
785

786 293

787
788 294 4.1. Stratigraphy
789

790 295 Detailed stratigraphic descriptions and diagrams have been previously
791
792 296 published (Punwong et al., 2012; 2013; 2013b). There were no abrupt
793
794 297 stratigraphic boundaries between the units; they were gradational in all ten cores.
795
796 298 The basal unit of BNR and CNR in the northern Rufiji Delta was comprised of
797
798 299 organic matter and silt (Punwong et al., 2012). Organic matter amount, including
799
800 300 root fragments, increased towards the top of the cores where wood and bark
801
802 301 fragments were also present.
803

804
805 302 In the three cores retrieved from Makoba Bay, the deepest sediment was
806
807 303 grey silt with some shell fragments (Punwong et al., 2013b). In cores AMAK-1
808
809 304 and BMAK-1 the silt unit was overlain by a peat unit containing woody root
810
811 305 fragments and fine sand. Sand was found in the uppermost unit of all three cores.
812

813 306 The basal unit of A-UU-1, B-UU-1 C-UU-1 sediment cores from Unguja
814
815 307 Ukuu was grey sand and silt with silt as the basal unit in C-UU-4 (Punwong et al.,
816
817 308 2013a). All basal units were overlain by peat with woody root fragments. Some
818
819 309 small shell fragments were also found in this unit in A-UU-1 and B-UU-1. Peat
820
821 310 layers with sand and small fragments of woody plant roots alternated with organic
822
823 311 sand layers throughout the sediment column in all four cores. Sand containing
824
825 312 small fragments of woody plant root formed the top unit of B-UU-1, C-UU-1, and
826
827 313 C-UU-4 while silt characterised the top unit of A-UU-1.
828

829
830 314

831
832 315 4.2. Pollen analysis and vegetation survey
833
834
835
836
837
838
839
840

841
842
843
844 316 Fossil pollen and spores were identified and placed into five main
845
846 317 ecological groups: mangroves, back mangroves, terrestrial herbaceous,
847
848 318 pteridophytes and unidentifiable pollen; the first two (mangroves, back
849
850 319 mangroves), denote a tolerance to sea-water inundation (Punwong et al., 2012;
851
852 320 2013a; 2013b). Terrestrial taxa consisted solely of terrestrial herbaceous plants
853
854 321 such as grasses and sedges that are not tolerant of salinity. An understanding of
855
856 322 the contemporary mangrove species within the zones is used to underpin the
857
858 323 interpretation of ecosystem and environmental changes through the fossil record.
859
860
861 324 Nine mangrove species found in Tanzania within a zonation scheme developed
862
863 325 through a combination of Watson's (1928) and Santisuk's (1983) inundation
864
865 326 classes (mangroves and back mangroves) and field-based observations of modern
866
867 327 ecological occurrences of mangrove taxa (Figure 2a) (Punwong et al., 2012;
868
869 328 2013a; 2013b) are therefore used as a modern analogue of mangrove pollen to
870
871 329 interpret sea level. Low mangrove diversities and a linear relationship between
872
873 330 contemporary mangrove habitat and inundation frequency negates the need for the
874
875 331 use of transfer functions (Ellison, 1989; Engelhart et al., 2007).

877
878 332 Contemporary vegetation assemblages observed in the field based on
879
880 333 Watson and Santisuk (1928) classes revealed a distinct vertical relationship with
881
882 334 present sea level. The altitude of the upper and lower limits of the mangrove areas
883
884 335 was +1.67 m to +3.47 m mean tide level (MTL) in the northern Rufiji Delta, -1.63
885
886 336 m to +1.47 m MTL in Makoba Bay, and -0.03 m to +1.87 m MTL at Unguja
887
888 337 Ukuu. The altitudinal variation of the upper and lower limits of the mangrove
889
890 338 areas at the three sites is due to different mangrove systems and environmental
891
892 339 settings. In the northern Rufiji Delta, an estuarine mangrove ecosystem exists
893
894 340 while at Unguja Ukuu and Makoba Bay, fringe mangroves with less freshwater

901
902
903
904 341 input are found. For Makoba Bay we acknowledge it is unusual for mangroves to
905
906 342 grow at -1.63 m MTL and is most likely caused by the geomorphology of the tidal
907
908 343 creek system that allows seaward mangrove species, e.g. *Sonneratia alba*, to
909
910 344 colonise altitudes below MTL.

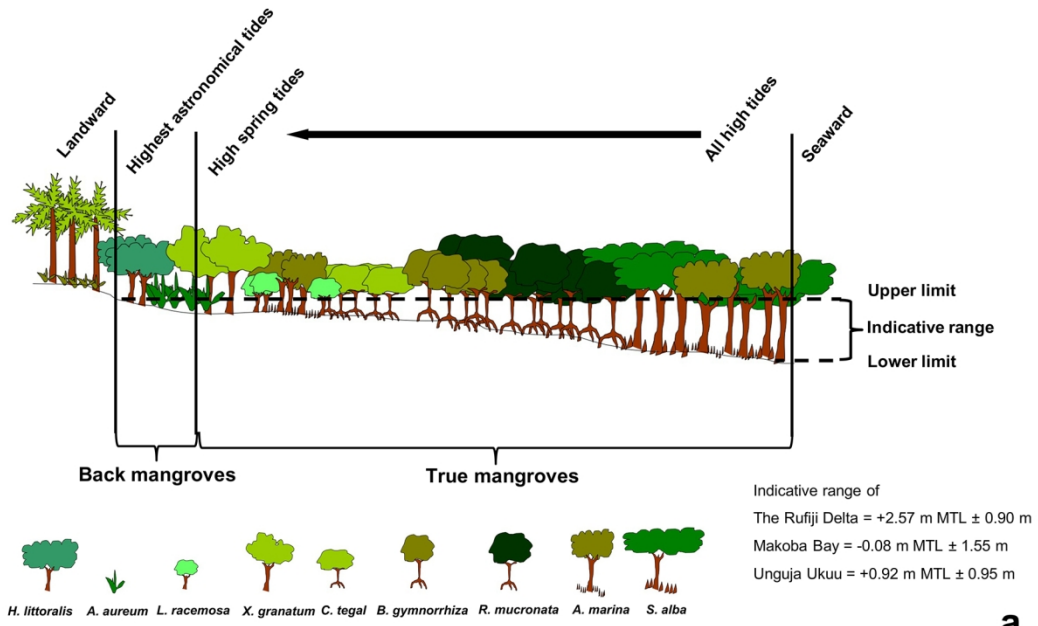
912 345 The indices of pollen association (Davis, 1984) and correlation between
913
914 346 the contemporary mangrove pollen records and contemporary vegetation showed
915
916 347 that fossil mangrove pollen in Zanzibar have a close correlation between
917
918 348 representivity in pollen spectra and the actual vegetation and can be used to
919
920 349 reconstruct coastal ecosystem dynamics (Punwong et al., 2013a; 2013b).
921
922
923 350 Strikingly, there are some notable changes between the percentages of *Sonneratia*
924
925 351 *alba* and *Bruguiera/Ceriops* pollen throughout Zanzibar cores. At the present-day
926
927 352 *Sonneratia alba* and *Bruguiera/Ceriops* appear at different altitudes; *Sonneratia*
928
929 353 *alba* occurs in the lower intertidal zone whilst *Bruguiera* and *Ceriops* occur at
930
931 354 higher intertidal areas. The relative pollen ratios of
932
933 355 *Sonneratia*:(*Bruguiera/Ceriops*) (S/BC ratio) and *Sonneratia*:*Rhizophora* (S/R
934
935 356 ratio) of the surface samples from each vegetation plot vary with altitudinal
936
937 357 gradient (Table 2). An increase in the ratios of S/BC and S/R indicates a decrease
938
939 358 in altitude of the mangrove ecosystem and associated sea level (Table 2). These
940
941 359 ratios are applied to infer the mangrove altitude shift within the upper and lower
942
943 360 altitudinal limits of the Makoba Bay and Unguja Ukuu study areas as a modern
944
945 361 analogue of altitude mangrove classes (Table 2). In Makoba, the S/BC ratios of
946
947 362 5.4 – 22.8 and the S/R ratios of 0.37 – 2.29 represent lower intertidal mangroves;
948
949 363 the S/BC ratios of 0.2 – 5.4 and the S/R ratios of 0.04 – 2.29 represent middle
950
951 364 intertidal mangroves; the S/BC ratios of 0 – 0.2 and S/R ratios of 0 – 0.04
952
953 365 represent higher intertidal mangroves. At Unguja Ukuu, the S/BC ratios of 0.17 –
954
955
956
957
958
959
960

961
962
963
964 366 2.23 and the S/R ratios of 0.20– 0.59 represent lower intertidal mangroves; the
965
966 367 S/BC ratios of 0 – 0.17 and the S/R ratios of 0 – 0.20 represent higher intertidal
967
968 368 mangroves.

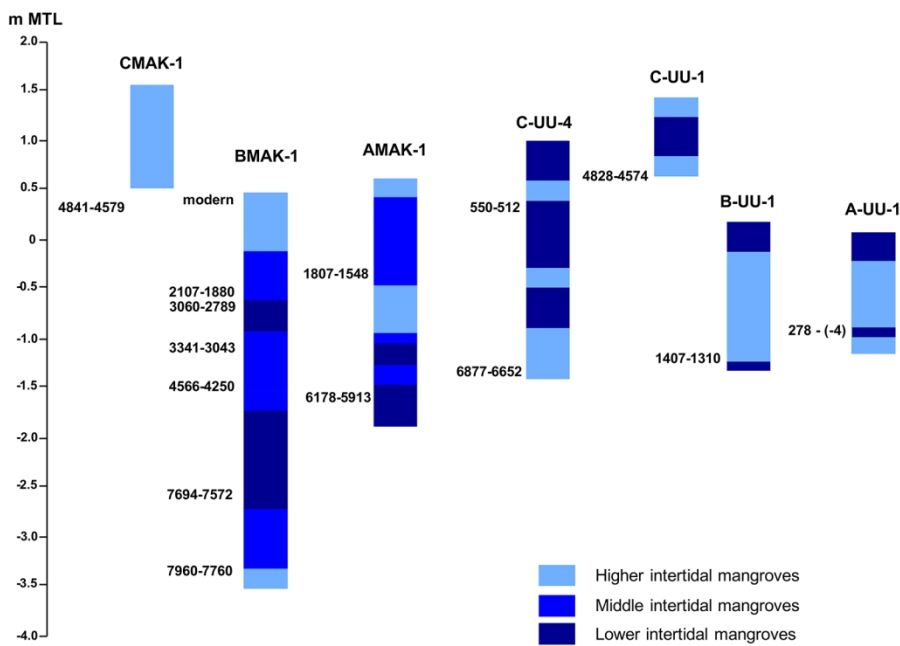
969
970 369 Therefore, the pollen biostratigraphy as used in this study allows
971
972 370 correlation between horizons using the S/BC and S/R ratios of the surface samples
973
974 371 within the eighteen vegetation plots that were calculated and used to characterise
975
976 372 the mangrove position of the reconstructed past mangrove ecosystems. This
977
978 373 information is applied to the dated samples (Figure 2b).

979
980
981 374
982
983
984
985
986
987
988
989
990
991
992
993
994
995
996
997
998
999
1000
1001
1002
1003
1004
1005
1006
1007
1008
1009
1010
1011
1012
1013
1014
1015
1016
1017
1018
1019
1020

1021
1022
1023
1024
1025
1026
1027
1028
1029
1030
1031
1032
1033
1034
1035
1036
1037
1038
1039
1040
1041
1042
1043
1044
1045
1046
1047
1048
1049
1050
1051
1052
1053
1054
1055
1056
1057
1058
1059
1060
1061
1062
1063
1064
1065
1066
1067
1068
1069
1070
1071
1072
1073
1074
1075
1076
1077
1078
1079
1080



a



b

375

376 Figure 2. (a) Summary cross section showing typical mangrove zonation and
377 response of this to RSL change in Tanzania developed from Watson's (1928) and
378 Santisuk's (1983) inundation classes and field observations with its indicative
379 range. Figure 2. (b) Biostratigraphy of core sites from Makoba Bay and Unguja
380 Ukuu showing paleoenvironmental interpretation in terms of mangrove position

1081
1082
1083
1084 as lower, middle, higher inferred from the ratios of S/BC and S/R. All ages are in
1085
1086
1087
1088
1089
1090
1091
1092
1093
1094
1095
1096
1097
1098
1099
1100
1101
1102
1103
1104
1105
1106
1107
1108
1109
1110
1111
1112
1113
1114
1115
1116
1117
1118
1119
1120
1121
1122
1123
1124
1125
1126
1127
1128
1129
1130
1131
1132
1133
1134
1135
1136
1137
1138
1139
1140

Site	Core	Altitude (m MTL)	¹⁴ C yr BP	(2σ) Calibrated age range yr BP	Indicative meaning (m MTL) derived from full range of mangrove	RSL (m MTL) derived from full range of mangroves	Mangrove classes with altitudinal range (interpolated from Fig. 2b)	Indicative meaning (m MTL) derived from pollen ratios	RSL (m MTL) derived from pollen ratios	Decompaction correction	Sea-level tendency
Northern Rufiji Delta	ANR	1.61	392 ± 30	493-324							
	BNR	3.22	> 1950 A.D.								
		2.95	Failure to make graphite								
		2.34	4167 ± 30	4821-4453	2.57 ± 0.9	-0.23 ± 0.9	n/a	n/a	n/a	1.03	rise
		0.61	4751 ± 30	5579-5318	2.57 ± 0.9	-1.96 ± 0.9	n/a	n/a	n/a	0.51	rise
	CNR	-0.96	4931 ± 30	5711-5486	2.57 ± 0.9	-3.59 ± 0.9	n/a	n/a	n/a	0.02	rise
		2.33	> 1950 A.D.								
		1.06	884 ± 31	799-680	2.57 ± 0.9	-1.51 ± 0.9	n/a	n/a	n/a	0.62	fall
	-0.97	1292 ± 30	1264-1071	2.57 ± 0.9	-3.54 ± 0.9	n/a	n/a	n/a	0.02	fall	
Makoba Bay	AMAK-1	-0.37*	1803 ± 36	1807-1548	-0.08 ± 1.55	-0.29 ± 1.55	Middle intertidal (-1.14)-0.57	-0.08 ± 0.86	-0.29 ± 0.86	0.46	rise
		-0.41	1615 ± 24	1525-1385							
		-1.55*	5290 ± 38	6178-5913	-0.08 ± 1.55	-1.47 ± 1.55	Lower intertidal (-1.61) - (-1.14)	-0.08 ± 0.23	-1.47 ± 0.23	0.11	fall
		-1.56	5078 ± 26	5892-5659							
	BMAK-1	0.39*	Modern		-0.08 ± 1.55	0.47 ± 1.55	Higher intertidal 0.57-1.51	-0.08 ± 0.47	0.47 ± 0.47	1.19	fall
		-0.54	3111 ± 24	3362-3167							
	BMAK-1	-0.55*	2072 ± 35	2107-1880	-0.08 ± 1.55	-0.47 ± 1.55	Middle intertidal (-1.14)-0.57	-0.08 ± 0.86	-0.47 ± 0.86	0.91	fall
		-0.64	1543 ± 25	1477-1305							
		-1.16	1695 ± 50	1692-1408							
		-1.17*	3053 ± 37	3341-3043	-0.08 ± 1.55	-1.09 ± 1.55	Middle intertidal (-1.14)-0.57	-0.08 ± 0.86	-1.09 ± 0.86	0.73	rise
		-1.53	309 ± 23	443-289							
		-1.54*	4024 ± 40	4566-4250	-0.08 ± 1.55	-1.46 ± 1.55	Middle intertidal (-1.14)-0.57	-0.08 ± 0.86	-1.46 ± 0.86	0.61	rise
	CMAK-1	-2.78	6878 ± 36	7735-7582							
		-2.79*	6847 ± 39	7694-7572	-0.08 ± 1.55	-2.7 ± 1.55	Low intertidal (-1.61) - (-1.14)	-0.08 ± 0.23	-2.70 ± 0.23	0.24	rise
		-3.52*	7092 ± 38	7960-7760	-0.08 ± 1.55	-3.46 ± 1.55	Middle intertidal (-1.14)-0.57	-0.08 ± 0.86	-3.46 ± 0.86	0.01	rise
		-3.54	7202 ± 30	8025-7872							
Unguja Ukuu	A-UU-1	-0.84	169 ± 22	278(-4)	0.92 ± 0.95	-1.76 ± 0.95	Lower intertidal 0.01-0.21	0.92 ± 0.10	-1.76 ± 0.10	0.17	fall
	B-UU-1	-1.24	1534 ± 23	1407-1310	0.92 ± 0.95	-2.16 ± 0.95	Higher intertidal 0.21-1.91	0.92 ± 0.85	-2.16 ± 0.85	0.04	fall
	C-UU-1	0.57	4211 ± 25	4828-4574	0.92 ± 0.95	-0.35 ± 0.95	Lower intertidal 0.01-0.21	0.92 ± 0.10	-0.35 ± 0.10	0.09	rise
	C-UU-4	0.59	>1950 AD								
		0.39	560 ± 19	550-512	0.92 ± 0.95	-0.53 ± 0.95	Lower intertidal 0.01-0.21	0.92 ± 0.10	-0.53 ± 0.10	0.47	fall
		-1.29	5973 ± 36	6877-6652	0.92 ± 0.95	-2.21 ± 0.95	Higher intertidal 0.21-1.91	0.92 ± 0.85	-2.21 ± 0.85	0.02	rise

383

384

385 Table 1. List of radiocarbon dates derived from bulk samples and organic
386 concentrates (marked with asterisks) from three sites. The calibrated ages are
387 shown using the Shcal04 curve (McCormac et al., 2004) within the software

1141
 1142
 1143
 1144 388 OxCal v4.10 Bronk-Ramsey (2009). RSL dates are also depicted using the
 1145
 1146 389 indicative range derived from the upper and lower limits of modern mangrove
 1147
 1148 390 vegetation and altitudinal error derived from the full range of mangroves for the
 1149
 1150 391 Rufiji Delta and from the pollen ratios for Makoba and Unguja Ukuu.

Site	Plot	Altitude of plot MTL (m)	Altitudinal range of mangrove classes	S/BC ratio	Range of S/BC ratios	S/R ratio	Range of S/R ratios	Mangrove classes
Makoba Bay	AMAK-3	-1.61	(-1.61) - (-1.14)	22.8	5.4-22.8	2.29	0.37-2.29	Lower intertidal
	AMAK-2	-1.14		5.4		0.37		
	BMAK-3	-0.55	(-1.14) - 0.57	1.3	0.2-5.4	0.07	0.04-2.29	Middle intertidal
	BMAK-2	-0.05		0.2		0.04		
	BMAK-1	0.42		0.2		0.05		
	AMAK-1	0.57		0.2		0.09		
	CMAK-3	1.01	0.57-1.51	0	0-0.2	0	0-0.04	Higher intertidal
	CMAK-1	1.48		0		0		
CMAK-2	1.51	0		0				
Unguja Ukuu	A-UU-3	0.01	0.01-0.21	2.23	0.17-2.23	0.59	0.20-0.59	Lower intertidal
	A-UU-1	0.07		0.88		0.20		
	B-UU-1	0.14		0.72		0.25		
	A-UU-2	0.21		0.17		0.33		
	B-UU-2	0.86	0.21-1.91	0.04	0-0.17	0.16	0-0.20	Higher intertidal
	B-UU-3	0.99		0.04		0.08		
	C-UU-1	1.35		0.02		0.05		
	C-UU-3	1.89		0		0		
	C-UU-2	1.91		0		0		

1152
 1153
 1154
 1155
 1156
 1157
 1158
 1159
 1160
 1161
 1162
 1163
 1164 392
 1165
 1166 393 Table 2. Vegetation plots of Makoba Bay and Unguja Ukuu showing
 1167
 1168 394 *Sonneratia/(Bruguiera/Ceriops)* (S/BC) and *Sonneratia/Rhizophora* (S/R) ratios
 1169
 1170 395 of surface samples developed from Punwong et al. (2013a; 2013b). The ranges of
 1171
 1172 396 ratios show the modern altitudinal range and are applied to infer the mangrove
 1173
 1174 397 position of sediment in core as modern analogue of lower intertidal, middle
 1175
 1176 398 intertidal, higher intertidal mangrove classes of the area with respect to altitude.

1178 399 1180 400 4.3. Chronology

1181
 1182
 1183 401 Nine radiocarbon dates were obtained from the northern Rufiji Delta
 1184
 1185 402 (Table 1). The radiocarbon dates indicate sedimentary hiatuses in the upper part of
 1186
 1187 403 BNR between 46 cm (4821- 4453 cal yr BP) and 19 cm (modern deposition) and
 1188
 1189 404 between 242 cm (799 - 680 cal yr BP) and 115 cm (modern deposition) in CNR.
 1190
 1191 405 The dates from 19 cm (BNR) and 115 cm (CNR) are therefore rejected for RSL
 1192
 1193 406 reconstruction. In ANR there is no pollen record between the depths of 115-150

1201
1202
1203
1204 407 cm. The date from 128 cm of ANR is therefore not applicable for RSL
1205
1206 408 reconstruction.

1207
1208 409 Eleven radiocarbon dates on bulk sediment were obtained from Makoba
1209
1210 410 Bay (Table 1). The radiocarbon dates from cores BMAK-1 (96 and 195 cm) and
1211
1212 411 CMAK-1 (107 and 172 cm) demonstrate age reversals. Despite their potential,
1213
1214 412 mangrove peats are notoriously difficult to date with age reversals common in
1215
1216 413 radiocarbon dated sequences, and modern ages often being reported from samples
1217
1218 414 collected several decimeters below the ground surface (e.g. Woodroffe and
1219
1220 415 Horton, 2005). The likely causes of these dating problems are reworking of
1221
1222 416 mangrove sediments through root penetration introducing younger carbon lower
1223
1224 417 down in the sediment profile and mixing of older sediments within the upper unit
1225
1226 418 (Punwong et al., 2013b; Woodroffe et al., 2015a). The nine dates obtained from
1227
1228 419 the organic concentrates reveal a coherent chronology and logical age-depth
1229
1230 420 relationship suggesting reliable dates for AMAK-1 and BMAK-1 (Woodroffe et
1231
1232 421 al., 2015a). It would therefore appear that the source of contamination, such as the
1233
1234 422 penetration of mangrove roots into the sediment matrix and bioturbation at depth,
1235
1236 423 taking younger carbon down the core (Punwong et al., 2013b; Woodroffe et al.,
1237
1238 424 2015a). We therefore reject the dates on bulk sediments from the cores AMAK-1,
1239
1240 425 BMAK-1 and the two reversed dates (at 107 and 172 cm) of CMAK-1 and use the
1241
1242 426 organic concentrate dates for RSL reconstruction. In CMAK-1, there is no pollen
1243
1244 427 record between the depths of 105-174 cm. The date from 130 cm of CMAK-1 is
1245
1246 428 therefore not used for RSL reconstruction.

1247
1248
1249 429 Six radiocarbon dates were obtained from Unguja Ukuu (Table 1). The
1250
1251 430 radiocarbon date from core C-UU-4 (42 cm) records modern age deposition,
1252
1253
1254
1255
1256
1257
1258
1259
1260

1261
1262
1263
1264 431 probably due to contamination (as described above) and this date is therefore
1265
1266 432 rejected for RSL reconstruction.

1267
1268 433

1269 434 4.4. RSL and compaction

1270
1272 435 In order to reconstruct RSL changes using mangrove sediments, the upper
1273
1274 436 and lower limits of mangrove vegetation with reference to the mean tide level
1275
1276 437 (MTL) is used in order to establish an indicative range for mangroves following
1277
1278 438 the approach of Woodroffe et al. (2015b) and Hijma et al. (2015). The indicative
1279
1280 439 ranges for mangrove sediments are $+2.57 \text{ m MTL} \pm 0.90 \text{ m}$ in the northern Rufiji
1281
1282
1283 440 Delta, $-0.08 \text{ m MTL} \pm 1.55 \text{ m}$ in Makoba Bay and $+0.92 \text{ m MTL} \pm 0.95 \text{ m}$ in
1284
1285 441 Unguja Ukuu (Table 1; Figure 2a). To reduce the vertical error, where detailed
1286
1287 442 contemporary vegetation pollen studies were undertaken in Makoba Bay and
1288
1289 443 Unguja Ukuu, we use the pollen ratios of S/BC and S/R to calculate the altitudinal
1290
1291 444 ranges of RSL (as described in 4.2 Pollen analysis and vegetation survey). For
1292
1293 445 example, the radiocarbon date of 1807-1548 cal yr BP occurs at the depth of 0.94
1294
1295 446 m in AMAK-1 from Makoba Bay; using the pollen ratios of S/BC and S/R
1296
1297 447 derived from contemporary pollen studies, it is possible that the vegetation at the
1298
1299 448 depth of 0.94 m represent a middle-intertidal mangrove association (Figure 2b). If
1300
1301 449 this is related to MTL using the vegetation plot data, the vertical error of the date
1302
1303 450 becomes $\pm 0.86 \text{ m}$ derived from the vertical range of the middle-intertidal
1304
1305 451 mangrove that is -1.14 m MTL and $+0.57 \text{ m MTL}$ (Table 1 and 2). The indicative
1306
1307 452 range derived from the upper and lower limit of mangrove vegetation in Makoba
1308
1309 453 Bay is -0.08 m MTL and therefore the indicative range of RSL from the date is -
1310
1311 454 $0.08 \text{ m MTL} \pm 0.86 \text{ m}$ (Table 1).

1312
1313
1314
1315
1316
1317
1318
1319
1320

1321
1322
1323
1324 455 Sediments are susceptible to post-depositional compaction (Bird et al.,
1325
1326 456 2004; Horton and Shennan, 2009). A compaction factor for the mangrove
1327
1328 457 sediment was estimated by comparing the dry bulk density of a compacted sample
1329
1330 458 with the modern sediment sample and found to range from 17-31% (Bird et al.,
1331
1332 459 2004). As this geotechnical technique is beyond the scope of study, the worst-case
1333
1334 460 compaction scenario of Bird et al. (2004) of 31% was adopted for the
1335
1336 461 decompaction correction below the depth dated (Table 1). For example, at the
1337
1338 462 depth 1.07 m of BNR that is 4.50 m in total length, the compaction of mangrove
1339
1340 463 sediment below this depth would be 1.0633 m (31% of 4.50 – 1.07 m) and would
1341
1342 464 be applied to the vertical error in an upward direction. This approach has also
1343
1344 465 been used in mangrove sea-level reconstructions from mangrove deposits in the
1345
1346 466 Seychelles (Woodroffe et al., 2015b).

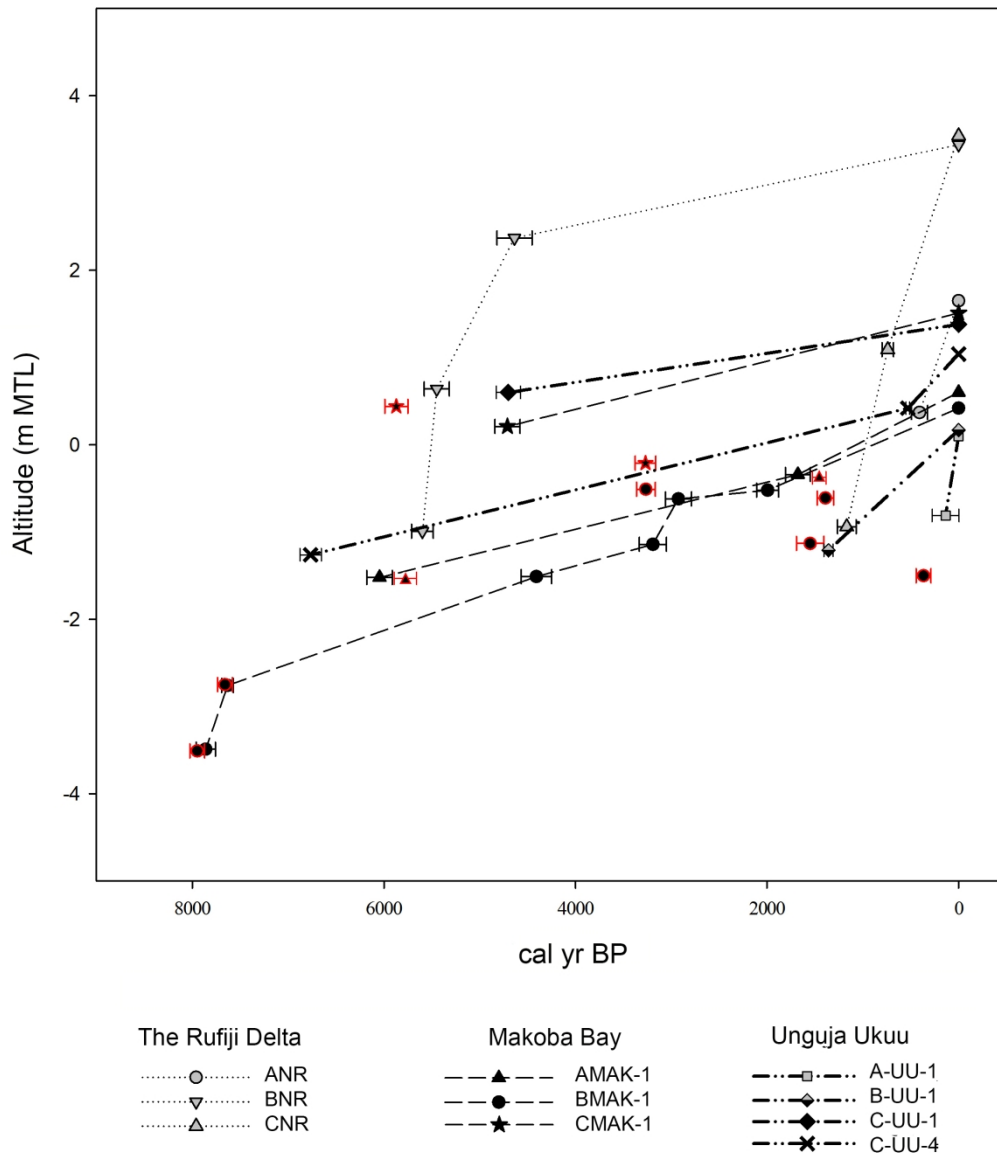
1347
1348
1349 467 Vertical errors also include compaction caused by the coring equipment (\pm
1350
1351 468 0.04 m) (Woodroffe, 2006), levelling errors (\pm 0.051 m), and the vertical range of
1352
1353 469 the radiocarbon date (\pm 0.005 m). Sea-level tendency for each RSL reconstruction
1354
1355 470 is determined (Table 1) by using a combination of stratigraphy and the trend of
1356
1357 471 mangrove pollen-based interpretation from each coring site (Figure 2b).

1358
1359
1360 472

1361 1362 473 5. Interpretation and discussion

1363
1364 474 Age-depth plots of the cores indicated that the basal age for each core
1365
1366 475 ranged from ~ 7900 cal yr BP (BMAK-1 of Makoba Bay) to ~100 cal yr BP (A-
1367
1368 476 UU-1 of Unguja Ukuu). A comparison of sedimentation rates showed great
1369
1370 477 variation between the Rufiji Delta and Zanzibar sites (Figure 3). Although the
1371
1372 478 chronology is problematic, it would appear that the sedimentation rate of between
1373
1374 479 2.1-10.9 mm cal yr⁻¹ for the Rufiji Delta was considerably higher than that for

1381
1382
1383
1384 480 Makoba Bay and Unguja Ukuu (0.3-6.6 mm cal yr⁻¹). This enhanced
1385
1386 481 sedimentation rate is probably due to the nature of the deltaic mangrove setting
1387
1388 482 with river discharge transporting sediment from the wider Rufiji catchment to be
1389
1390 483 deposited into the Rufiji Delta (Semesi, 1992; Fisher et al., 1994). The variation in
1391
1392 484 sedimentation rates results in different altitudinal ranges of the mangrove areas at
1393
1394 485 the three locations with freshwater input, sediment supply and progradation
1395
1396 486 having significantly more effect in the Rufiji Delta than at the Zanzibar sites.
1397
1398 487 However, given site-specific responses of mangroves relative to sea level, when
1399
1400 488 sites are combined, they provide regional RSL reconstruction.
1401
1402
1403 489
1404
1405
1406
1407
1408
1409
1410
1411
1412
1413
1414
1415
1416
1417
1418
1419
1420
1421
1422
1423
1424
1425
1426
1427
1428
1429
1430
1431
1432
1433
1434
1435
1436
1437
1438
1439
1440



490

491 Figure 3. Comparative age-depth plots including rejected dates (in red edge) for
 492 the cores analysed in this study. Comparative age-depth (altitude) models for the
 493 cores analysed in this study. The top value against the zero origin (cal yr BP) on
 494 all such graphs except BMAK-1 does not necessarily represent present day
 495 deposition because of potential surface erosion.

496

497 5.1. Holocene mangrove dynamics

498
499
500

1501
1502
1503
1504 498 Combined palaeoecological records from the three locations provide a new
1505
1506 499 palaeoenvironmental sea-level synthesis from Tanzania where relatively little is
1507
1508 500 known about the Holocene mangrove dynamics. The records reveal that mangrove
1509
1510 501 ecosystems have not remained stable as they responded to wide scale
1511
1512 502 environmental changes and there are some site-specific responses to
1513
1514 503 environmental shifts. The results further our understanding of how mangrove
1515
1516 504 ecosystems reflect environmental variables, and shifts in these, that could help
1517
1518 505 assess resilience of coastal ecosystems under future climatic scenarios,
1519
1520 506 particularly sea-level rise (Ellison, 2015).

1522
1523 507 Early to mid Holocene

1525 508 The pollen record of BMAK-1 indicates that mangroves have been present
1526
1527 509 at Makoba Bay at -3.6 m below MTL since at least ~7900 cal yr BP (Figure 2b).
1528
1529 510 The ratios of S/BC and S/R suggest that the central core (BMAK-1) location was
1530
1531 511 colonised by higher intertidal mangroves (Figures 1f, 2b; Table 2) suggesting an
1532
1533 512 early Holocene RSL rise. A higher RSL rise was then recorded after this period
1534
1535 513 for a relatively short duration until ~7600 cal yr BP, as mangroves migrated
1536
1537 514 landward and this area supported middle intertidal mangrove taxa. RSL continued
1538
1539 515 to rise, as indicated by the ratios of mangrove pollen and the deposition of oyster
1540
1541 516 shells in BMAK-1b and AMAK-1. This marine transgression caused the
1542
1543 517 mangrove taxa at these two coring locations to migrate further landwards and
1544
1545 518 allowed mangroves to establish on the headland of Unguja Ukuu at -1.3 m MTL
1546
1547 519 as recorded ~6800 cal yr BP in C-UU-4. After this time, higher intertidal
1548
1549 520 mangroves recorded in C-UU-4 were replaced by lower intertidal mangrove taxa;
1550
1551 521 thus contributing to a body of evidence indicating that RSL continued to rise
1552
1553 522 during the mid Holocene (Camoin et al., 1997; 2004; Zinke et al., 2003; Norström
1554
1555
1556
1557
1558
1559
1560

1561
1562
1563
1564 523 et al., 2012). It should be noted that the pollen records from both sites in Zanzibar
1565
1566 524 reveals a similar age determination of 5600 cal yr BP and a similar pollen record,
1567
1568 525 lending support to the chronological and sea-level interpretation from BNR in the
1569
1570 526 northern Rufiji Delta (Punwong et al., 2012). The predominance of *R. mucronata*
1571
1572 527 pollen suggests that BNR was located in a low intertidal environment, a further
1573
1574 528 indication of a higher sea level relative to the present day. A mid Holocene RSL
1575
1576 529 rise possibly attained a higher altitude after 4700 cal yr BP resulting in higher
1577
1578 530 intertidal mangroves establishment at 0.5 m above MTL in CMAK-1 and higher
1579
1580 531 intertidal mangrove establishment at 0.6 m MTL in C-UU-1. This mid Holocene
1581
1582 532 RSL rise occurred until prior to ~4400 cal yr BP, when RSL started to fall as
1583
1584 533 indicated by the transition from lower intertidal to middle intertidal mangroves in
1585
1586 534 BMAK-1.

1587
1588
1589 535
1590
1591 536 Mid Holocene to the present day

1592
1593 537 After ~4400 cal yr BP mangrove ecosystem character varied between the
1594
1595 538 sites reflecting different RSL changes. A lower RSL is recorded in Makoba Bay
1596
1597 539 from ~4400 cal yr BP, as indicated by the change in mangrove composition from
1598
1599 540 lower to middle intertidal mangroves in BMAK-1 until ~3200 cal yr BP. This
1600
1601 541 period coincides with a regionally arid phase recorded across East Africa
1602
1603 542 commencing around 4500–4100 cal yr BP (Hassan, 1997; Bonnefille and Chalieu,
1604
1605 543 2000; Thompson et al., 2002; Marchant and Hooghiemstra, 2004; Kiage and Liu,
1606
1607 544 2006; Rijdsdijk et al., 2011; de Boer et al., 2015). After 3200 cal yr BP, and prior
1608
1609 545 to 2900 cal yr BP, a RSL rise occurred indicative of a change from middle to
1610
1611 546 lower intertidal mangroves. Mangrove composition subsequently changed to
1612
1613 547 middle intertidal mangroves in AMAK-1 and BMAK-1 (Figure 2b) suggesting a
1614
1615
1616
1617
1618
1619
1620

1621
1622
1623
1624 548 lower RSL as mangroves retreated seaward until the late Holocene ~2000-1700
1625
1626 549 cal yr BP. However, a sea-level rise is recorded at Unguja Ukuu as lower
1627
1628 550 intertidal mangroves occupied C-UU-1 and C-UU-4 after the mid Holocene until
1629
1630 551 ~500 cal yr BP. The apparent discrepancy in RSL between these two sites at
1631
1632 552 Unguja after 4400 to 1700 cal yr BP is probably due to local processes including
1633
1634 553 mangrove composition response to sediment input and/or erosion at the sites,
1635
1636 554 resulting in localised RSL changes.

1638
1639 555 The late Holocene RSL fall is recorded at all three sites. In Makoba Bay,
1640
1641 556 RSL fell until the present day, as suggested by the change of middle intertidal
1642
1643 557 mangroves to higher intertidal mangroves in AMAK-1 and BMAK-1. At Unguja
1644
1645 558 Ukuu, lower intertidal mangroves changed to higher intertidal mangroves after
1646
1647 559 1400 cal yr BP in B-UU-1. RSL probably continued falling in Unguja Ukuu, as
1648
1649 560 represented by the change from lower intertidal mangroves to higher intertidal
1650
1651 561 mangroves after ~500 cal yr BP in C-UU-4, and the presence of more intertidal
1652
1653 562 mangroves after ~100 cal yr BP in A-UU-1. In the Rufiji Delta, a reduction in
1654
1655 563 mangrove pollen and increase in back-mangrove and terrestrial grasses in the
1656
1657 564 landward site (CNR) after 1200 cal yr BP resulted in a shift of mangroves
1658
1659 565 seaward. RSL then fluctuated, as suggested by changes in the proportions of
1660
1661 566 mangroves, back-mangrove and terrestrial grasses until prior to 700 cal yr BP.
1662
1663 567 After 700 cal yr BP, RSL started to fall, as recorded by a gradual change from
1664
1665 568 mangroves characterised by *R. mucronata* to terrestrial vegetation, and a
1666
1667 569 replacement of mangroves by recent herbaceous taxa. However, changes from
1668
1669 570 higher intertidal mangroves to lower intertidal mangroves in A-UU-1, B-UU-1
1670
1671 571 and C-UU4 at Unguja Ukuu, corresponding to an increase in *A. marina* at the top
1672
1673
1674
1675
1676
1677
1678
1679
1680

1681
1682
1683
1684 572 of ANR, are likely to represent a signal of sea-level rise during the last few
1685
1686 573 hundred years.

1687
1688 574

1689
1690 575 5.2. Sea-level reconstruction

1692 576 The pollen evidence from the Rufiji Delta, Makoba Bay and Unguja Ukuu
1693
1694 577 can be used to reconstruct the Holocene RSL from Tanzania using the upper and
1695
1696 578 lower limits of mangrove vegetation and shift in recognisable salinity tolerance
1697
1698 579 zones of the mangrove ecosystem. The RSL derived from the pollen ratios within
1699
1700 580 the vegetation plots can refine vertical errors (Figure 4). Regardless of site-
1701
1702 581 specific characteristics, it should be noted that all three sites provide evidence for
1703
1704 582 a phase of early-mid Holocene RSL rise and late Holocene RSL fluctuation. The
1705
1706 583 composite RSL curve shows that RSL rise occurred from around 7900 cal yr BP.
1707
1708 584 It is possible that RSL rose and was potentially higher than present at ~4700-4600
1709
1710 585 cal yr BP. However, when the sites are compared (Figure 4), variations in the rate
1711
1712 586 of sea level rise are noted. In the northern Rufiji Delta, the higher sedimentation
1713
1714 587 rates are probably due to the large freshwater and terrestrial inputs to the system.

1717 588 The general trend of the early to mid Holocene RSL rise (Figure 4)
1718
1719 589 appears to be in agreement with RSL trends from other locations such as the
1720
1721 590 mainland coast and offshore islands in the Southwest Indian Ocean (Colonna et
1722
1723 591 al., 1996; Camoin et al., 1997; 2004; Zinke et al., 2000; Compton, 2001; Ramsay
1724
1725 592 and Cooper, 2002; Zinke et al., 2003).

1727 593 The proposed higher than present sea level at around 4700-4600 cal yr BP
1728
1729 594 recorded in Tanzania indicates a similar trend to that recorded from South Africa
1730
1731 595 (Compton, 2001; Ramsay and Cooper, 2002) (Figure 4). The mid Holocene RSL
1732
1733 596 rise in Tanzania is also comparable to a marine transgression phase in
1734
1735
1736
1737
1738
1739
1740

1741
1742
1743
1744 597 Mozambique (Norström et al., 2012) where a highstand is recorded ~6600-6300
1745
1746 598 cal yr BP. The mid Holocene transgression is well represented from the Southern
1747
1748 599 Hemisphere in far-field locations (Isla, 1989) relating to three possible causes
1749
1750 600 including meltwater from late glacial ice sheets (Lambeck and Nakada, 1990;
1751
1752 601 Fleming et al., 1998) and/or the Holocene melting of ice sheets from Antarctica,
1753
1754 602 Greenland and mountain glaciers during the early Holocene until 5000 cal yr BP
1755
1756 603 (Milne et al., 2005).

1758
1759 604 Evidence from Mauritius, Mayotte and Réunion Island (Camoin et al.,
1760
1761 605 1997; 2004; Zinke et al., 2003) suggest no mid Holocene highstand occurred at
1762
1763 606 these locations. The differences between the records from the islands and
1764
1765 607 Tanzania may result from hydro-isostatic influences relating to the differences in
1766
1767 608 the geographical locations of the Tanzanian coast and the islands (Clark et al.,
1768
1769 609 1978). The Holocene highstand at small offshore islands is likely to be less
1770
1771 610 marked than at the continental margins due to the effects of continental levering
1772
1773 611 (Lambeck and Nakada, 1990; Mitrovica and Milne, 2002; Milne and Mitrovica,
1774
1775 612 2008). However, the highstand recorded from South Africa is likely to be higher
1776
1777
1778 613 than the potential maximum transgression at ~4700 cal yr BP and 4600 cal yr BP
1779
1780 614 in Tanzania (Compton, 2001; Ramsay and Cooper, 2002). In addition to eustatic
1781
1782 615 changes, a combination of various factors such as hydro-isostasy, thermal
1783
1784 616 expansion of sea water caused by warmer ocean temperatures in subtropical
1785
1786 617 latitudes (Ramsay, 1995, Woodroffe and Horton, 2005), and the steric expansion
1787
1788 618 of sea water (Ramsay, 1995; Compton, 2001) may also be considered as factors
1789
1790 619 enhancing the highstand altitude in South Africa.

1792
1793 620 RSL fell from 4600 cal yr BP to 4400 cal yr BP. After 4400 cal yr BP,
1794
1795 621 RSL slightly rose until ~2000 cal yr BP. The RSL record at this time from
1796
1797
1798
1799
1800

1801
1802
1803
1804 622 Tanzania correlates well with records from South Africa (Ramsay and Cooper,
1805
1806 623 2002) and also corresponds with a possible marine transgression with a highstand
1807
1808 624 from Macassa Bay (Mozambique) between 4000 - 1100 cal yr BP (Norström et
1809
1810 625 al., 2012). The pollen records from Makoba Bay and C-UU-1 and C-UU-4 of
1811
1812 626 Unguja Ukuu indicate that mangrove development continued after the mid
1813
1814 627 Holocene RSL rise indicating a sustained higher level that did not fall until the
1815
1816 628 late Holocene ~2000 cal yr BP. This may have allowed suitable conditions for
1817
1818 629 mangroves to establish at A-UU-1 and B-UU-1 and may correspond to the
1819
1820 630 progradation of beach plains that is recorded in Zanzibar (Arthurton, 2003).

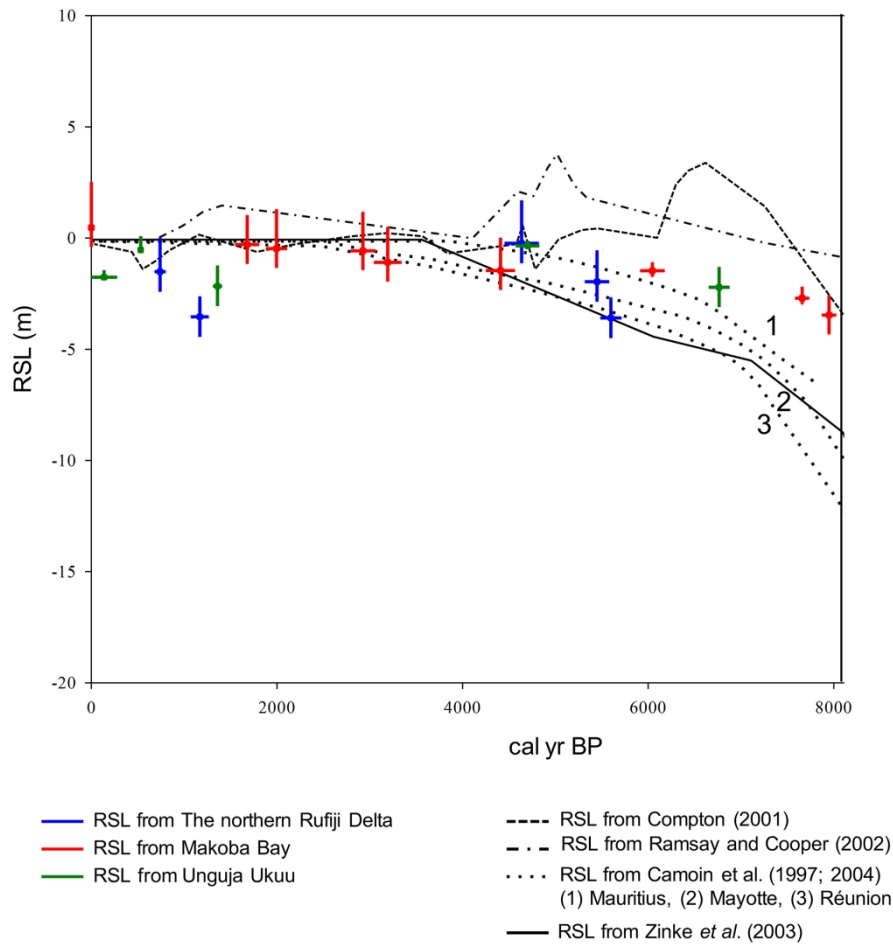
1821
1822
1823 631 The late Holocene RSL record after 2000 cal yr BP until 100 cal yr BP
1824
1825 632 correlates well with the RSL records from South Africa (Compton, 2001; Ramsay
1826
1827 633 and Cooper, 2002) and Mozambique (Norström et al., 2012) (Figure 4). A lower
1828
1829 634 sea level occurred in Tanzania until 1400 - 1200 cal yr BP; this RSL fall is also
1830
1831 635 recorded in northeastern South Africa ~1400 cal yr BP to the present (Ramsay and
1832
1833 636 Cooper, 2002). We acknowledged that potential sea-level fall would correspond to
1834
1835 637 climatically cold phases and sea-level rise to warm phases, as a result of the
1836
1837 638 glacial eustasy (Oerlemans, 2001). Changes in rainfall can also cause local
1838
1839 639 eustatic sea-level changes (Mörner, 1996). However, easternmost East Africa
1840
1841 640 experienced drought during the Medieval Warm Period (MWP) (900 - 700 cal yr
1842
1843 641 BP) and wet conditions during the Little Ice Age (LIA) (700 - 100 cal yr BP)
1844
1845 642 (Verchuren et al., 2000). These phases are contrast with our records of sea-level
1846
1847 643 transgression after 1200 - 500 cal yr BP and sea-level regression from 500 - 100
1848
1849 644 cal yr BP. Archaeological sites in Unguja Ukuu indicate that RSL was
1850
1851 645 approximately -0.5 m below the present level between ~1300 - 1000 cal yr BP
1852
1853 646 (Mörner, 1992). This is in good agreement with the reconstruction from the three
1854
1855
1856
1857
1858
1859
1860

1861
1862
1863
1864 647 sites studied suggesting RSL did not attain present sea level between 1400-1200
1865
1866 648 cal yr BP (Figure 4).

1868 649 A further RSL rise occurred after 1200 to ~700 - 500 cal yr BP and it is
1869
1870 650 likely that RSL was below the present sea level. This concurs with records from
1871
1872 651 ruins in southeastern Tanzania (Kilwa) suggesting RSL was about -1 m below the
1873
1874 652 present level between 800- 600 cal yr BP (Mörner, 1992). After this period, RSL
1875
1876 653 fell until ~100 cal yr BP when sea level was lower than the present day. This is in
1877
1878 654 good agreement with a study of raised terraces along the Kenyan coast indicating
1879
1880 655 that RSL started to fall 500 years ago (Åse, 1978; 1981). In contrast, data from
1881
1882 656 Mozambique (Norström et al., 2012) and southern Langebaan Lagoon in South
1883
1884 657 Africa (Compton, 2001) show somewhat conflicting results from the Tanzanian
1885
1886 658 data indicating RSL fell after 1200 cal yr BP. After 100 cal yr BP, RSL rose until
1887
1888 659 the present day corresponding to the onset of recent sea-level rise from the 19th
1889
1890 660 century (Stocker et al., 2013) as recorded in Kenya between 1986-2002 (Kibue,
1891
1892 661 2006). However, a recent sea-level fall was observed in Zanzibar between 1985-
1893
1894 662 2001 (Permanent Service for Mean Sea Level) before rising trend was observed to
1895
1896 663 the present day. In addition, it should be noted that Makoba and Unguja Ukuu
1897
1898 664 which all are on the west cost of Unguja Island and separated by 40 km shows
1899
1900 665 different RSL especially during the last 2000 years probably due to local
1901
1902 666 processes, such as changes in sediment input and/or erosion at the sites.

1906 667 Difficulties encountered in dating suggest additional records and
1907
1908 668 chronological control using dating of pollen concentrates is required to determine
1909
1910 669 a high-resolution record of mid Holocene sea level and environmental changes.
1911
1912 670 Although the evidence from Tanzania demonstrates the site-specific nature of
1913
1914 671 responses of mangroves to RSL changes, it does provide a valuable contribution

1921
 1922
 1923
 1924 672 to patterns of Holocene RSL from “far-field” locations. There is great potential to
 1925
 1926 673 scale up the type of investigation presented here to other coastal mangrove sites
 1927
 1928 674 across East Africa, as well as offshore islands. Such an extension to this study
 1929
 1930 675 would provide an unprecedented regional record of environmental and sea-level
 1931
 1932 676 changes from a far-field region and allow us to distinguish large and meso-scale
 1933
 1934
 1935 677 regional signals against site-specific responses across East Africa.



678
 679 Figure 4. RSL reconstructions from this study along the Tanzanian coast plotted
 680 alongside RSL curves from the southwest Indian Ocean region

681
 682 6. Conclusions

1981
1982
1983
1984 683 A reconstruction of Holocene RSL has been derived for coastal Tanzania
1985
1986 684 from mangrove ecosystem changes from three sites. The ratios of
1987
1988 685 *Sonneratia:(Bruguiera/Ceriops)* and *Sonneratia:Rhizophora* derived from the
1989
1990 686 pollen-vegetation-altitude relationships can be used to interpret mangrove
1991
1992 687 dynamics and refine the vertical errors of RSL changes derived from mangrove
1993
1994 688 sediments. Although the results in part demonstrate the site-specific shifts in the
1995
1996 689 upper and lower limits of mangroves relative to sea level, due to responses of
1997
1998 690 sediment input and/or erosion at the three sites, they do provide evidence for
1999
2000 691 Holocene RSL fluctuations coherent across coastal Tanzania. An early-mid to mid
2001
2002 692 Holocene RSL rise occurred from ~ 7900 cal yr BP prior to ~4700-4600 cal yr BP
2003
2004 693 when RSL was potentially higher than the present. This period is followed by a
2005
2006 694 lower RSL until 4400 cal yr BP when RSL rose until ~2000 cal yr BP.
2007
2008 695 Subsequently, late Holocene RSL fluctuations were characterised by RSL rise
2009
2010 696 recorded at ~700 - 500 cal yr BP before falling below the present level at ~100 cal
2011
2012 697 yr BP. There is evidence of a more recent RSL rise during the last centuries. The
2013
2014 698 Tanzanian RSL curve indicates a similar trend to the mid Holocene RSL record
2015
2016 699 from South Africa, probably related to similar hydro-isostatic conditions
2017
2018 700 representing the apparent Holocene highstand at continental margins due to the
2019
2020 701 effects of continental levering. The RSL fall recorded during the last 500 years is
2021
2022 702 in good agreement with the records from the Kenyan coast, although data from
2023
2024 703 Mozambique and the Langebaan Lagoon in South Africa indicate RSL fell after
2025
2026 704 1200 cal yr BP. The difficulties of developing a reliable chronology from
2027
2028 705 mangrove environments have previously precluded extensive use of these
2029
2030 706 sediment archives for reconstructing RSL changes. Organic concentrate dating
2031
2032 707 applied on some of the samples presented here can provide a reliable chronology
2033
2034
2035
2036
2037
2038
2039
2040

2041
2042
2043
2044 708 allowing these far-field locations to be fully investigated and used as a proxy for
2045
2046 709 reconstructing eustatic sea-level changes. Site-specific signals of RSL change,
2047
2048 710 mangrove response to this and the need to further constrain the pollen-vegetation-
2049
2050 711 environmental relationships all emphasise the need for further research along the
2051
2052 712 East African coast, as well as other “far-field” locations, so that the full potential
2053
2054 713 of the mangrove sedimentary sea-level archive can be fully realised.
2055

2056 714

2058 715 Acknowledgements

2060 716 This work was carried out as a part of doctoral thesis at the University of
2061
2062 717 York. Thanks are extended to Mr William Kindeketa and Rebecca Newman for
2063
2064 718 their support and assistance throughout the fieldwork. We would like to thank the
2065
2066 719 Palynology & Palaeobotany Section, National Museums of Kenya for lending us
2067
2068 720 the coring equipment necessary for fieldwork and laboratory work, WWF-
2069
2070 721 Tanzania for providing logistical support for the fieldwork in Rufiji Delta and Mr
2071
2072 722 Benson Kimeu, Survey/GIS Technician from The British Institute in Eastern
2073
2074 723 Africa for conducting the elevation survey. I am grateful to Professor Antony
2075
2076 724 Long, Dr. Sarah Woodroffe and Dr. Sanpisa Sritrairat for their constructive
2077
2078 725 comments on earlier versions of this manuscript. The radiocarbon dates on the
2079
2080 726 organic concentrates was funded through NERC Radiocarbon Facility Allocation
2081
2082 727 1608.0312. This study was supported by The Royal Thai Government Scholarship
2083
2084 728 and the Development and Promotion Science and Technology Talents project.
2085
2086 729

2088 729

2090 730 References

2092 731
2093
2094
2095
2096
2097
2098
2099
2100

2101
2102
2103
2104
2105
2106
2107
2108
2109
2110
2111
2112
2113
2114
2115
2116
2117
2118
2119
2120
2121
2122
2123
2124
2125
2126
2127
2128
2129
2130
2131
2132
2133
2134
2135
2136
2137
2138
2139
2140
2141
2142
2143
2144
2145
2146
2147
2148
2149
2150
2151
2152
2153
2154
2155
2156
2157
2158
2159
2160

732 Admiralty Tide Tables, 2014. NP203 Admiralty Tide Tables (ATT) Volume 3,
733 Indian Ocean and South China Sea (including Tidal Stream Tables).
734 Hydrographer to the Navy. Admiralty Hydrography Department. 365 pp.
735 Arthurton, R.S., Brampton, A.H., Kaaya, C.Z., Mohamed, S.K., 1999. Late
736 Quaternary coastal stratigraphy on a platform-fringed tropical coast- a case study
737 from Zanzibar, Tanzania. *Journal of Coastal Research* 15, 635-644.
738 Arthurton, R., 2003. The fringing reef coasts of eastern Africa-present processes
739 in their long-term context. *Western Indian Ocean Journal Marine Science* 2 (1), 1-
740 13.
741 Åse, L.E., 1978. Preliminary Report on Studies of Shore Displacement at the
742 Southern Coast of Kenya. *Geografiska Annaler, Series A, Physical Geography*,
743 60, 3/4, 209-221.
744 Åse, L.E., 1981. Studies of Shores and Shore Displacement on the Southern Coast
745 of Kenya. Especially in the Kilifi District. *Geografiska Annaler, Series A*,
746 *Physical Geography*, 63, 3/4, 303-310.
747 Baker, R.G., Haworth, R., Flood, P., 2001. Inter-tidal fixed indicators of former
748 Holocene sea levels in Australia: a summary of sites and a review of methods and
749 models. *Quaternary International* 83–85, 257–273.
750 Banerjee, P.K., 2000. Holocene and Late Pleistocene relative sea level
751 fluctuations along the east coast of India. *Marine Geology* 167, 243–260.
752 Bird, M. I., L. K. Fifield, S. Chua, Goh, B., 2004. Calculating sediment
753 compaction for radiocarbon dating of intertidal sediments. *Radiocarbon* 46(1),
754 421–435.

- 2161
2162
2163
2164 755 Bird, M.I., Fifield, L.K., Teh, T.S., Chang, C.H., Shirlaw, N., Lambeck, K., 2007.
2165
2166 756 An inflection in the rate of early-mid Holocene eustatic sea-level rise: A new sea-
2167
2168 757 level curve from Singapore. *Estuarine, Coastal and Shelf Science* 71, 523–536.
2169
2170 758 Blasco, F., Saenger, P., Janodet, E. 1996. Mangroves as indicators of coastal
2171
2172 759 change. *Catena* 27, 167–178.
2173
2174 760 Bonnefille, R., Chalieu, F., 2000. Pollen-inferred precipitation time-series from
2175
2176 761 equatorial mountains, Africa, the last 40 kyr BP. *Global Planet Change* 26, 25–50.
2177
2178 762 Bronk-Ramsey, C., 2009. OxCal Program v4.10. Oxford Radiocarbon Accelerator
2179
2180 763 Unit, Oxford.
2181
2182 764 Camoin, G.F., Colonna, M., Montaggioni, L.F., Casanova, J., Faure, G.,
2183
2184 765 Thomassin, B.A., 1997. Holocene sea level changes and reef development in the
2185
2186 766 southwestern Indian Ocean. *Coral Reefs* 16 (4), 247–259.
2187
2188 767 Camoin, G.F., Montaggioni, L.F., Braithwaite, C.J.R., 2004. Late glacial to post
2189
2190 768 glacial sea levels in the Western Indian Ocean. *Marine Geology* 206, 119–146.
2191
2192 769 Clark, J.A., Farrell, W.E., Peltier, W.R., 1978. Global changes in post glacial sea
2193
2194 770 level: a numerical calculation. *Quaternary Research* 9, 265–287.
2195
2196 771 Cohen, M.C.L., Behling, H., Lara, R.J., 2005. Amazonian mangrove dynamics
2197
2198 772 during the last millennium: The relative sea-level and the Little Ice Age. *Review*
2199
2200 773 *of Palaeobotany and Palynology* 136, 93-108.
2201
2202 774 Colonna, M., Casanova, J., Dullo, W.C., Camoin, G., 1997. Sea-level changes and
2203
2204 775 $\delta^{18}\text{O}$ record for the past 34,000 yr from Mayotte Reef, Indian Ocean.
2205
2206 776 *Oceanographic Literature Review* 44(7), 693–693.
2207
2208 777 Compton, J.S., 2001. Holocene sea-level fluctuations inferred from the evolution
2209
2210 778 of depositional environments of the southern Langebaan Lagoon salt marsh, South
2211
2212 779 Africa. *The Holocene* 11(4), 395–405.
2213
2214
2215
2216
2217
2218
2219
2220

- 2221
2222
2223
2224 780 Davis, O.K., 1984. Pollen frequencies reflect vegetation patterns in a Great Basin
2225
2226 781 (U.S.A.) mountain range. *Review of Palaeobotany and Palynology* 40, 295–315.
2227
2228 782 de Boer, E.J., Vélez, M.I., Rijdsdijk, K.F., de Louw, P.G., Vernimmen, T.J., Visser,
2229
2230 783 P.M., Tjallingii, R. and Hooghiemstra, H., 2015. A deadly cocktail: How a
2231
2232 784 drought around 4200 cal. yr BP caused mass mortality events at the infamous
2233
2234 785 ‘dodo swamp’ in Mauritius. *The Holocene*, 25(5), 758–771.
2235
2236 786 Ellison, A.M., Farnsworth, E.J., 2001. Mangrove communities. In: Bertness,
2237
2238 787 M.D., Gaines, S.D., Hay, M.E. (Eds.). *Marine Community Ecology*. Sinauer
2239
2240 788 Associates, Sunderland, MA. pp. 423–442.
2241
2242
2243 789 Ellison, J.C., 1989. Pollen analysis of mangrove sediments as a sea level
2244
2245 790 indicator: assessment from Tongatapu, Tonga. *Palaeogeography,*
2246
2247 791 *Palaeoclimatology, Palaeoecology* 74: 327–341.
2248
2249 792 Ellison, J.C., 2005. Holocene palynology and sea-level change in two estuaries in
2250
2251 793 Southern Irian Jaya. *Palaeogeography and Palaeoclimatology*. 220, 291–309.
2252
2253 794 Ellison, J.C., 2008. Long-term retrospection on mangrove development using
2254
2255 795 sediment cores and pollen analysis: A review. *Aquatic Botany* 89, 93–104.
2256
2257 796 Ellison, J.C., 2015. Vulnerability assessment of mangroves to climate change and
2258
2259 797 sea-level rise impacts. *Wetlands Ecology and Management*, 23(2), 115–137.
2260
2261 798 Engelhart, S.E., Horton, B.P., Roberts, D.H., Bryant, C.L., Corbett, D.R., 2007.
2262
2263 799 Mangrove pollen of Indonesia and its suitability as a sea level indicator. *Marine*
2264
2265 800 *Geology* 242, 65-81.
2266
2267 801 Fairbanks, R.G., 1989. A 17,000-year glacio-eustatic sea level record: influence of
2268
2269 802 glacial melting rates on the Younger Dryas event and deep- ocean circulation.
2270
2271 803 *Nature* 342, 639–642.
2272
2273
2274
2275
2276
2277
2278
2279
2280

2281
2282
2283
2284
2285
2286
2287
2288
2289
2290
2291
2292
2293
2294
2295
2296
2297
2298
2299
2300
2301
2302
2303
2304
2305
2306
2307
2308
2309
2310
2311
2312
2313
2314
2315
2316
2317
2318
2319
2320
2321
2322
2323
2324
2325
2326
2327
2328
2329
2330
2331
2332
2333
2334
2335
2336
2337
2338
2339
2340

804 Fisher, P. R., Dyer, K., Semesi, A. 1994. Rufiji Delta hydrodynamics research
805 program, Final report: Characteristic circulation and sedimentation in the Rufiji
806 delta, Tanzania. Frontier-Tanzania Technical report No. 13. The Society for
807 Environment Exploration. U.K.

808 Fleming, K., Johnston, P., Zwartz, D., Yokoyama, Y., Lambeck, K., Chappell, J.,
809 1998. Refining the eustatic sea-level curve since the Last Glacial Maximum using
810 far-and intermediate-field sites. *Earth and Planetary Science Letters* 163, 327–
811 342.

812 Francis, J. 1992. Physical processes in the Rufiji delta and their possible
813 implications on the mangrove ecosystem. *Hydrobiologia* 247, 173–179.

814 Gasse, F., 2000. Hydrological changes in the African tropics since the Last
815 Glacial Maximum. *Quaternary Science Reviews* 19, 189–211.

816 Gehrels, R., Long, A., 2008. Sea level is not level: the case for a new approach to
817 predicting UK sea-level rise. *Geography* 93(1), 11–16.

818 Gilman, E.L., Ellison, J., Duke, N.C. and Field, C., 2008. Threats to mangroves
819 from climate change and adaptation options: A review. *Aquatic Botany* 89(2),
820 237–250.

821 Goudie, A. S., 1996. Climate: past and present. In: Adams, W.A., Goudie, A.S.,
822 Orme, A.R. (eds) *The physical geography of Africa*. Oxford University Press,
823 New York, pp 34–59

824 Hait, A. K., Behling, H., 2009. Holocene mangrove and coastal environmental
825 changes in the western Ganga–Brahmaputra Delta, India. *Vegetation History and*
826 *Archaeobotany* 18, 159–169.

827 Hanebuth, T., Stattegger, K., Grootes, P.M., 2000. Rapid Flooding of the Sunda
828 Shelf: A Late-Glacial Sea-Level Record. *Science* 288, 1033–1035.

2341
2342
2343
2344
2345
2346
2347
2348
2349
2350
2351
2352
2353
2354
2355
2356
2357
2358
2359
2360
2361
2362
2363
2364
2365
2366
2367
2368
2369
2370
2371
2372
2373
2374
2375
2376
2377
2378
2379
2380
2381
2382
2383
2384
2385
2386
2387
2388
2389
2390
2391
2392
2393
2394
2395
2396
2397
2398
2399
2400

829 Hassan, F.A., 1997. Holocene Palaeoclimates of Africa. *African Archaeological*
830 *Review* 14(4), 213–230.

831 Hijma, M., Engelhart, S.E., Törnqvist, T.E., Horton, B.P., Hu, P. and Hill, D.F.,
832 2015. A protocol for a geological sea-level database. *Handbook of Sea-Level*
833 *Research*, edited by: Shennan, I., Long, AJ, and Horton, BP, Wiley Blackwell, pp.
834 536–553.

835 Horton, B.P., Benjamin, P., Gibbard, L.G., Milne, M., Morley, R.J.,
836 Purintavaragul, C. and Stargardt, J.M., 2005. Holocene sea levels and
837 palaeoenvironments, Malay-Thai Peninsula, Southeast Asia. *The Holocene* 15,
838 1199–1213.

839 Isla, F.I., 1989. Holocene sea-level fluctuation in the Southern Hemisphere.
840 *Quaternary Science Reviews* 8, 359–368.

841 Jaritz, W., Ruder, J., B, Schlenker, B., 1977. Das Quartar im Küstengebiet von
842 Mocambique und seine Schwermineralführung. *Geologisches Jahrbuch, B*, 26: 3–
843 93.

844 Katupotha, J., Fujiwara, K., 1988. Holocene sea level change on the southwest
845 and south coasts of Sri Lanka. *Palaeogeography, Palaeoclimatology,*
846 *Palaeoecology* 68, 189–203.

847 Kiage, L.M., Liu, K., 2006. Late Quaternary paleoenvironmental changes in East
848 Africa: areview of multiproxy evidence from palynology, lake sediments, and
849 associated records. *Progress in Physical Geography* 30 (5), 633–658.

850 Kibue, A. M., 2006. Sea level measurement and analysis in the Western Indian
851 Ocean. National Report, Kenya.

852 Knopp, S., Mohammed, K.A., Simba Khamis, I., Mgeni, A.F., Stothard, J.R.,
853 Rollinson, D., Marti, H., Utzinger, J., 2008. Spatial distribution of soil-transmitted

- 2401
2402
2403
2404 854 helminths, including *Strongyloides stercoralis*, among children in Zanzibar.
2405
2406 855 Geospatial Health 3 (1), 47–56.
2407
2408 856 Lambeck, K., Nakada, M., 1990. Late Pleistocene and Holocene sea-level change
2409
2410 857 along the Australian coast. Palaeogeography, Palaeoclimatology, Palaeoecology
2411
2412 858 89, 143–176.
2413
2414 859 Lambeck, K., Rouby, H., Purcell, A., Sun, Y., Sambridge, M., 2014. Sea level and
2415
2416 860 global ice volumes from the Last Glacial Maximum to the Holocene. P Natl.
2417
2418 861 Acad. Sci. U. S. A. 111, 15296–15303.
2419
2420 862 Larcombe, P., Carter, R.M., Dye, J., Gagan, M.K., Johnson, D.P., 1995. New
2421
2422 863 evidence for episodic post-glacial sea-level rise, central Great Barrier Reef,
2423
2424 864 Australia. Marine Geology 127, 1–44.
2425
2426 865 Lewis, S.E., Sloss, C.R., Murray-Wallace, C.V., Woodroffe, C.D. and Smithers,
2427
2428 866 S.G., 2013. Post-glacial sea-level changes around the Australian margin: a review.
2429
2430 867 Quaternary Science Reviews, 74, pp. 115–138.
2431
2432 868 Machiwa, J.F., Hallberg, R.O., 1995. Flora and crabs in a mangrove forest partly
2433
2434 869 distorted by human activities. Zanzibar Ambio 24 (7–8), 492–496.
2435
2436 870 Mangora, M.M., Shalli, M.S., Semesi, I.S., Njana, M.A., Mwainunu, E.J., Otieno,
2437
2438 871 J.E., Ntibasubile, E., Mallya, H.C., Mukama, K., Wambura, M. and Chamuya,
2439
2440 872 N.A., 2016, January. Designing a mangrove research and demonstration forest in
2441
2442 873 the rufiji delta, Tanzania. In Proceedings of the 5th Interagency Conference on
2443
2444 874 Research in the Watersheds, pp. 190-192. US Department of Agriculture Forest
2445
2446 875 Service, Southern Research Station.
2447
2448 876 Marchant, R.A., Hooghiemstra, H., 2004. Rapid environmental change in Africa
2449
2450 877 and South American tropics around 4000 years before present. Earth Science
2451
2452 878 Reviews 66, 217–260.
2453
2454
2455
2456
2457
2458
2459
2460

- 2461
2462
2463
2464 879 Masalu, D.C.P., 2003. Challenges of coastal area management in coastal
2465
2466 880 developing countries—lessons from the proposed Rufiji Delta prawn farming
2467
2468 881 project, Tanzania. *Ocean Coastal Management* 46, 175–188.
2469
2470 882 McCormac, F.G., Hogg, A.G., Blackwell, P.G., Buck, C.E., Higham, T.F.G.,
2471
2472 883 Reimer, P.J., 2004. SHCal04 Southern Hemisphere Calibration, 0–11.0 cal kyr
2473
2474 884 BP. *Radiocarbon* 46(3), 1087–1092.
2475
2476 885 McIvor, A.L., Spencer, T., Möller, I. and Spalding, M., 2013. The response of
2477
2478 886 mangrove soil surface elevation to sea level rise. *Natural Coastal Protection*
2479
2480 887 Series: Report 3. Cambridge Coastal Research Unit Working Paper 42. The
2481
2482 888 Nature Conservancy and Wetlands International. 59 pp.
2483
2484 889 Milne, G., Long, A., Bassett, S., 2005. Modelling Holocene relative sea-level
2485
2486 890 observations from the Caribbean and South America. *Quaternary Science*
2487
2488 891 *Reviews* 24, 1183–1202.
2489
2490 892 Milne, G.A., Mitrovica, J.X., 2008. Searching for eustasy in deglacial sea-level
2491
2492 893 histories. *Quaternary Science Reviews* 27, 2292–2302.
2493
2494 894 Mitrovica, J.X., Peltier, W.R., 1991. On postglacial geoid subsidence over the
2495
2496 895 equatorial oceans. *Journal of Geophysical Research* 96, 20053–20071.
2497
2498 896 Mitrovica, J.X., Milne, G.A., 2002. On the origin of late Holocene sea-level
2499
2500 897 highstands within equatorial ocean basins. *Quaternary Science Reviews* 21, 2179–
2501
2502 898 2190.
2503
2504 899 Mörner, N., 1992. Ocean circulation, sea level changes and east African coastal
2505
2506 900 settlements. In Sinclair, P.J.J., and Juma, A., (Eds.). *Urban Origins in Eastern*
2507
2508 901 *Africa: Proceedings of the 1991 Workshop in Zanzibar*. Stockholm: Swedish
2509
2510 902 Central Board of National Antiquities, pp. 256–266.
2511
2512
2513
2514
2515
2516
2517
2518
2519
2520

2521
2522
2523
2524
2525
2526
2527
2528
2529
2530
2531
2532
2533
2534
2535
2536
2537
2538
2539
2540
2541
2542
2543
2544
2545
2546
2547
2548
2549
2550
2551
2552
2553
2554
2555
2556
2557
2558
2559
2560
2561
2562
2563
2564
2565
2566
2567
2568
2569
2570
2571
2572
2573
2574
2575
2576
2577
2578
2579
2580

903 Mörner, N.A., 1996. Global change and interaction of earth rotation, ocean
904 circulation and paleoclimate. *Anais da Academia Brasileira de Ciências*, 68, 77-
905 94.

906 Mwandya, A.W., Gullstrom, M., Andersson, M.H., Ohman, M.C., Mgya, Y.D.,
907 Bryceson, I., 2010. Spatial and seasonal variations of fish assemblages in
908 mangrove creek systems in Zanzibar (Tanzania). *Estuarine, Coastal and Shelf
909 Science* 89(4), 277–286.

910 Nicholson, S.E., 2001. Climatic and environmental change in Africa during the
911 last two centuries. *Climate research*, 17(2), 123-144.

912 Nshubemuki, L., 1993. Forestry resources in Tanzania’s wetlands: concepts and
913 potentials. *Wetlands of Tanzania*, 37–48.

914 Norström, E., Risberg, J., Gröndahl, H., Holmgren, K., Snowball, I., Mugabe, J.A.
915 Siteo, S.R., 2012. Coastal Paleo-environment and Sea-level Change at Macassa
916 Bay, Southern Mozambique, Since c 6600 Cal BP. *Quaternary International* 260,
917 153–163.

918 Oerlemans, J., 2001. *Glaciers and climate change*. Library of Congress
919 Cataloging-in-Publication Data.

920 Pirazzoli, P. A., Montaggioni, L. F., Salvat, B., & Faure, G., 1988. Late Holocene
921 sea level indicators from twelve atolls in the central and eastern Tuamotus (Pacific
922 Ocean). *Coral Reefs*, 7(2), 57–68.

923 Pirazzoli, P.A., 1991: *World Atlas of Holocene sea level changes*. Elsevier,
924 Amsterdam, 300 pp.

925 Prendergast, M.E., Rouby, H., Punwong, P., Marchant, R., Crowther, A.,
926 Kourampas, N., Shipton, C., Walsh, M., Lambeck, K. and Boivin, N.L., 2016.

- 2581
2582
2583
2584 927 Continental island formation and the archaeology of defaunation on Zanzibar,
2585
2586 928 eastern Africa. PLoS ONE 11(2): e0149565.
2587
2588 929 Punwong, P., Marchant, R., Selby, K., 2012. Holocene mangrove dynamics and
2589
2590 930 environmental change in the Rufiji Delta, Tanzania. *Vegetation History and*
2591
2592 931 *Archaeobotany* 22(5), 381–396.
2593
2594 932 Punwong, P., Marchant, R., Selby, K., 2013a. Holocene mangrove dynamics from
2595
2596 933 Unguja Ukuu, Zanzibar. *Quaternary International* 298, 4–19.
2597
2598 934 Punwong, P., Marchant, R., Selby, K., 2013b. Holocene mangrove dynamics in
2599
2600 935 Makoba Bay, Zanzibar. *Palaeogeography Palaeoclimatology Palaeoecology* 379–
2601
2602 936 380, 54–67.
2603
2604 937 Ramsay, P.J, 1995. 9000 years of sea-level change along the southern African
2605
2606 938 coastline. *Quaternary International* 31, 71–75.
2607
2608 939 Ramsay, P.J., Cooper, J. A. G., 2002. Late Quaternary Sea-Level Change in South
2609
2610 940 Africa. *Quaternary Research* 57, 82–90.
2611
2612 941 Richmond, M. D., Wilson, J. D. K., Mgaya, Y. D., Le Vay, L. 2002. An analysis
2613
2614 942 of smallholder opportunities in fisheries, coastal and related enterprises in the
2615
2616 943 floodplain and delta areas of the Rufiji River, Tanzania. *Rufiji Environment*
2617
2618 944 *Management Project Technical report* (25), 89 pp.
2619
2620 945 Rijdsdijk, K.F., Zinke, J., de Loux, P.G.B., Hume, J.P., van der Plicht, H.,
2621
2622 946 Hooghiemstra, H., Meijer, H.J.M., Vonhof, H., Porch, N., Florens, V., Baider, C.,
2623
2624 947 van Geel, B., Brinkkemper, J., Vernimmen, T., Janoo, A., 2011. Mid-Holocene
2625
2626 948 (4200 kyr BP) mass mortalities in Mauritius (Mascarenes): Insular vertebrates
2627
2628 949 resilient to climatic extremes but vulnerable to human impact. *The Holocene*, 1–
2629
2630 950 16.
2631
2632
2633
2634
2635
2636
2637
2638
2639
2640

2641
2642
2643
2644 951 Santisuk, T., 1983. Taxonomy and distribution of terrestrial trees and shrubs in
2645
2646 952 the mangrove formations in Thailand. *The Natural History Bulletin of the Siam*
2647
2648 953 *Society*. 5 (1), 63–91.
2649
2650 954 Schlüter, T., 1997. *Geology of East Africa*. Gebrüder Borntraeger, Berlin, 484 pp.
2651
2652 955 Semesi, A. K., 1992. The mangrove resource of the Rufiji delta, Tanzania. In:
2653
2654 956 Matiza T, Chabwela HN (Eds.) *Wetlands conservation conference for southern*
2655
2656 957 *Africa. Proceedings of the southern African development coordination conference*
2658
2659 958 *held in Gaborono, Botswana, 3–5 June 1991. Union Internationale pour la*
2660
2661 959 *Conservation de la Nature et de ses Ressources, Switzerland (UICN), Gland, pp*
2662
2663 960 *157–172.*
2664
2665 961 Shennan, I., Innes, J. B., Long, A. J., & Zong, Y. 1995. Late Devensian and
2666
2667 962 Holocene relative sea-level changes in northwestern Scotland: new data to test
2668
2669 963 existing models. *Quaternary International*, 26, 97–123.
2670
2671 964 Shunula, J.P., 2002. Public awareness, key to mangrove management and
2672
2673 965 conservation: the case of Zanzibar. *Trees* 16, 209–212.
2674
2675 966 Sloss, C. R., Murray-Wallace, C. V., & Jones, B. G., 2007. Holocene sea-level
2676
2677 967 change on the southeast coast of Australia: a review. *The Holocene*, 17(7), 999–
2678
2679 968 1014.
2680
2681 969 Stocker, T.F., Qin, D., Plattner, G.K., Tignor, M., Allen, S.K., Boschung, J.,
2682
2683 970 Nauels, A., Xia, Y., Bex, B. and Midgley, B.M., 2013. IPCC, 2013: climate
2684
2685 971 change 2013: the physical science basis. Contribution of working group I to the
2686
2687 972 fifth assessment report of the intergovernmental panel on climate change.
2688
2689 973 Thompson, L.G., Mosley-Thompson, E., Davis, M.E., Henderson, K.A., Brecher,
2690
2691 974 H.H., Zagorodnov, V.S., Mashiotta, T.A., Lin, P., Mikhaleiko, V.N., Hardy,

2641
2642
2643
2644
2645
2646
2647
2648
2649
2650
2651
2652
2653
2654
2655
2656
2657
2658
2659
2660
2661
2662
2663
2664
2665
2666
2667
2668
2669
2670
2671
2672
2673
2674
2675
2676
2677
2678
2679
2680
2681
2682
2683
2684
2685
2686
2687
2688
2689
2690
2691
2692
2693
2694
2695
2696
2697
2698
2699
2700

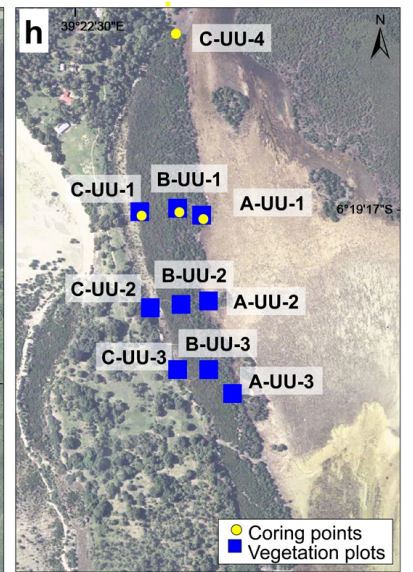
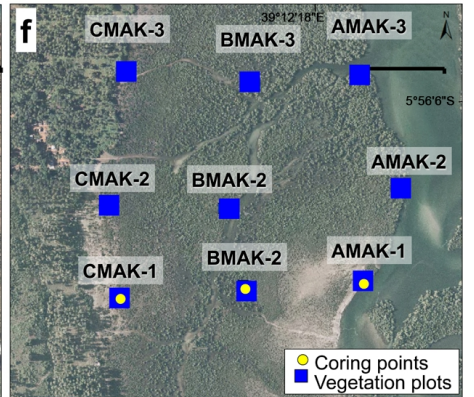
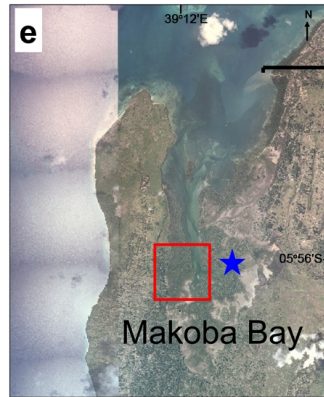
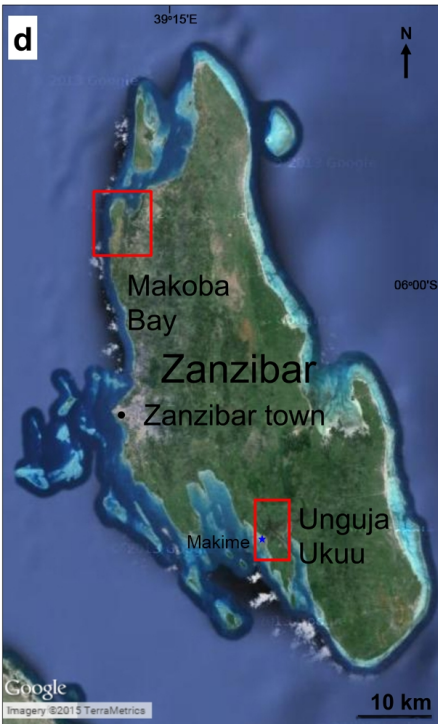
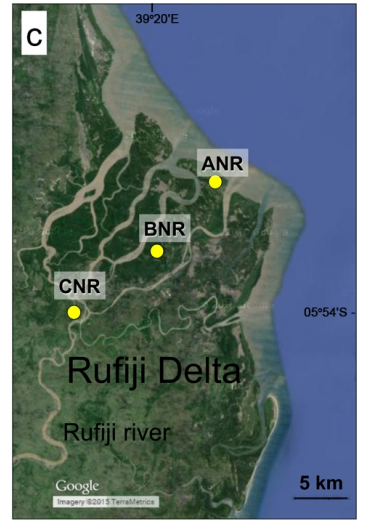
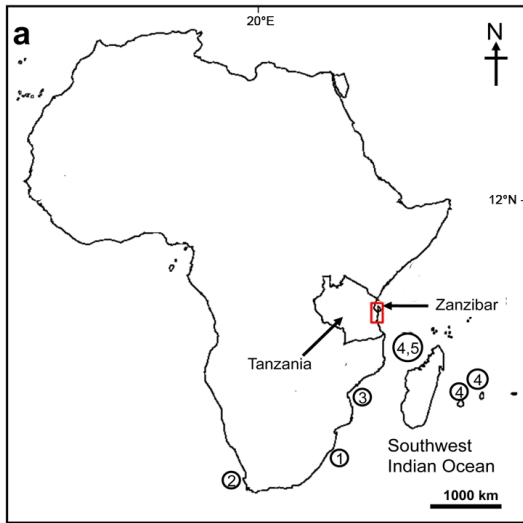
- 2701
2702
2703
2704 975 D.R., Beer, J., 2002. Kilimanjaro ice core records: evidence of Holocene climate
2705
2706 976 change in tropical Africa. *Science* 298, 589–593.
2707
2708 977 Tossou, M.G., Akoègninoua, A., Balloucheb, A., Sowunmic, M.A., Akpagana,
2709
2710 978 K., 2008. The history of the mangrove vegetation in Bénin during the Holocene:
2711
2712 979 A palynological study. *Journal of African Earth Sciences* 52, 167–174.
2713
2714 980 Vedel, V., Behling, H., Cohen, M., Lara, R., 2006. Holocene mangrove dynamics
2715
2716 981 and sea-level changes in northern Brazil, inferences from the Taperebal core in
2717
2718 982 northeastern Pará State. *Vegetation History and Archaeobotany* 15, 115–123.
2719
2720 983 Verschuren, D., Laird, K.R. and Cumming, B.F., 2000. Rainfall and drought in
2721
2722 984 equatorial east Africa during the past 1,100 years. *Nature*, 403(6768), 410-414.
2723
2724
2725 985 Watson, J. G. 1928. Mangrove forests of the Malay Peninsula. *Malayan Forest*
2726
2727 986 *Records* 6, 275 pp.
2728
2729 987 Woodroffe, C.D., Grindrod, J., 1991. Mangrove Biogeography: The Role of
2730
2731 988 Quaternary Environmental and Sea-Level Change. *Journal of Biogeography* 18,
2732
2733 989 479.
2734
2735 990 Woodroffe, S.A., Horton, BP, 2005. Holocene sea-level changes in the Indo-
2736
2737 991 Pacific. *Journal of Asian Earth Sciences* 25, 29–43.
2738
2739 992 Woodroffe, S.A., 2006. Holocene relative sea-level changes in Cleveland Bay,
2740
2741 993 North Queensland, Australia. PhD thesis, University of Durham, 155 pp.
2742
2743
2744 994 Woodroffe, S. A., Long, A.J., Punwong, P., Selby, K., Bryant, C.L., Marchant, R.,
2745
2746 995 2015a. Radiocarbon dating of mangrove sediments to constrain Holocene sea-
2747
2748 996 level change on Zanzibar in the Southwest Indian Ocean. *The Holocene* 25(5),
2749
2750 997 820-831.
2751
2752
2753
2754
2755
2756
2757
2758
2759
2760

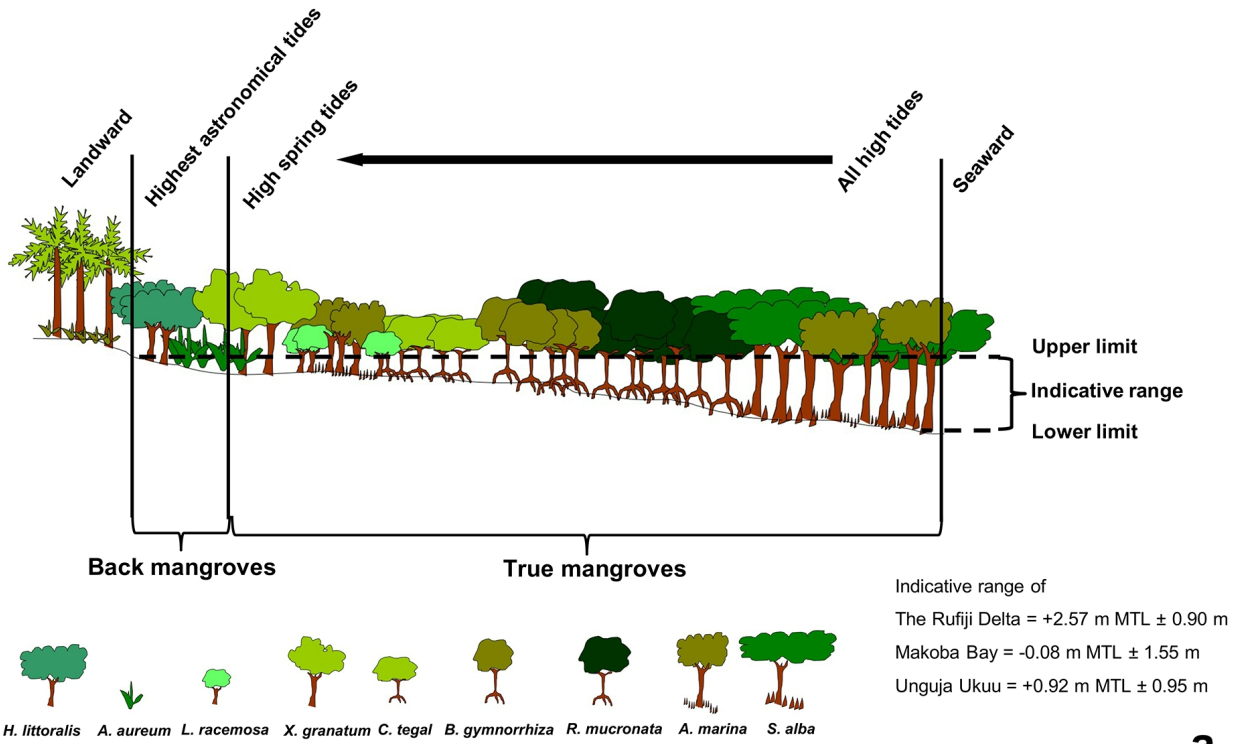
2761
2762
2763
2764
2765
2766
2767
2768
2769
2770
2771
2772
2773
2774
2775
2776
2777
2778
2779
2780
2781
2782
2783
2784
2785
2786
2787
2788
2789
2790
2791
2792
2793
2794
2795
2796
2797
2798
2799
2800
2801
2802
2803
2804
2805
2806
2807
2808
2809
2810
2811
2812
2813
2814
2815
2816
2817
2818
2819
2820

998 Woodroffe, S. A., Long, A. J., Milne, G. A., Bryant, C. L., & Thomas, A. L.
999 2015b. New constraints on late Holocene eustatic sea-level changes from Mahé,
1000 Seychelles. *Quaternary Science Reviews* 115, 1–16.

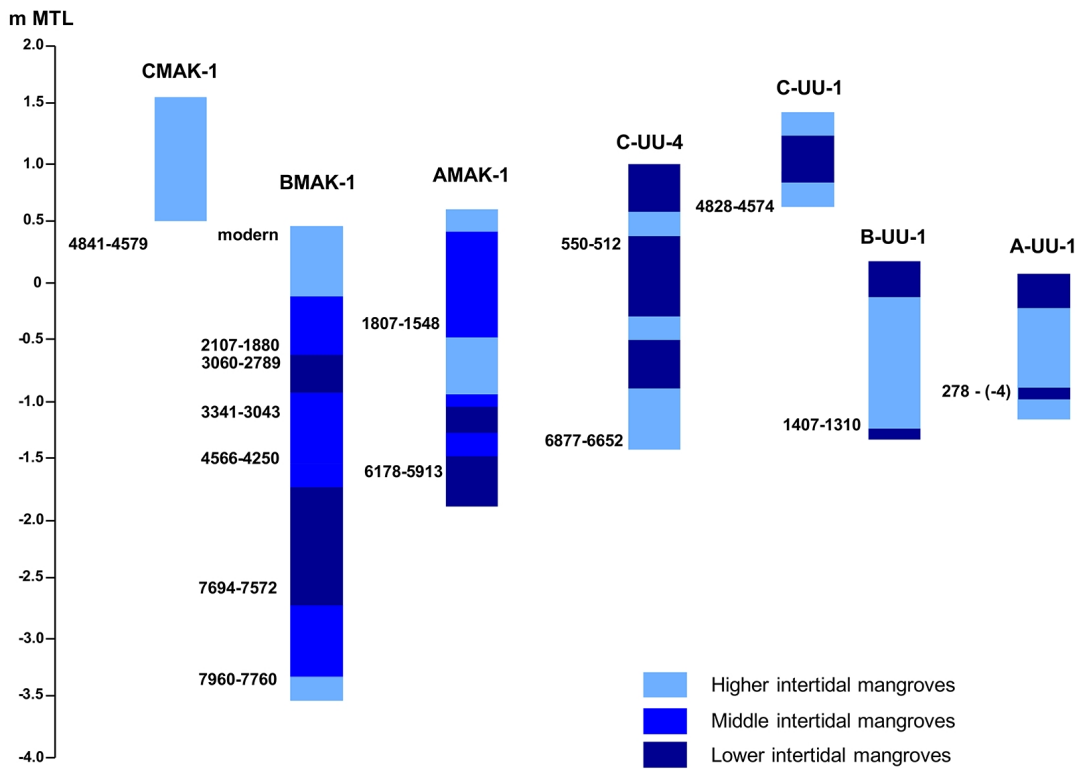
1001 Zinke, J., Reijmer, J.J.G., Dullo, W. C., Thomassin, B.A., 2000.
1002 Paleoenvironmental changes in the lagoon of Mayotte associated with the
1003 Holocene transgression. *Geolines* 11, 150–153.

1004 Zinke, J., Reijmer, J.J.G., Thomassin, B.A., Dullo, W. C., Grootes, P.M. and
1005 Erienkeuser, H., 2003. Postglacial flooding history of Mayotte Lagoon (Comoro
1006 Archipelago, southwest Indian Ocean). *Marine Geology*, 194 (3-4), 181–196.

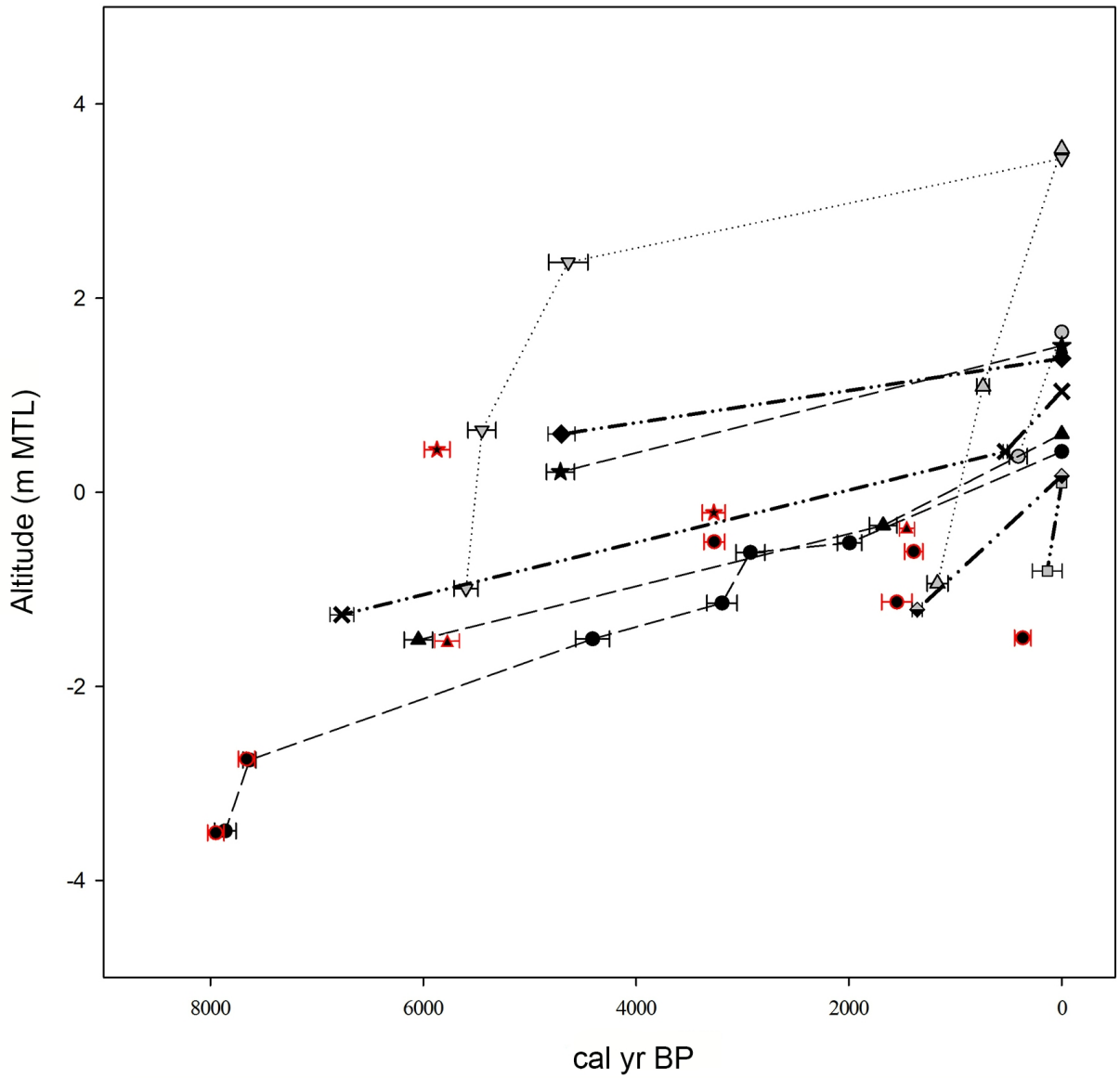




a



b



The Rufiji Delta

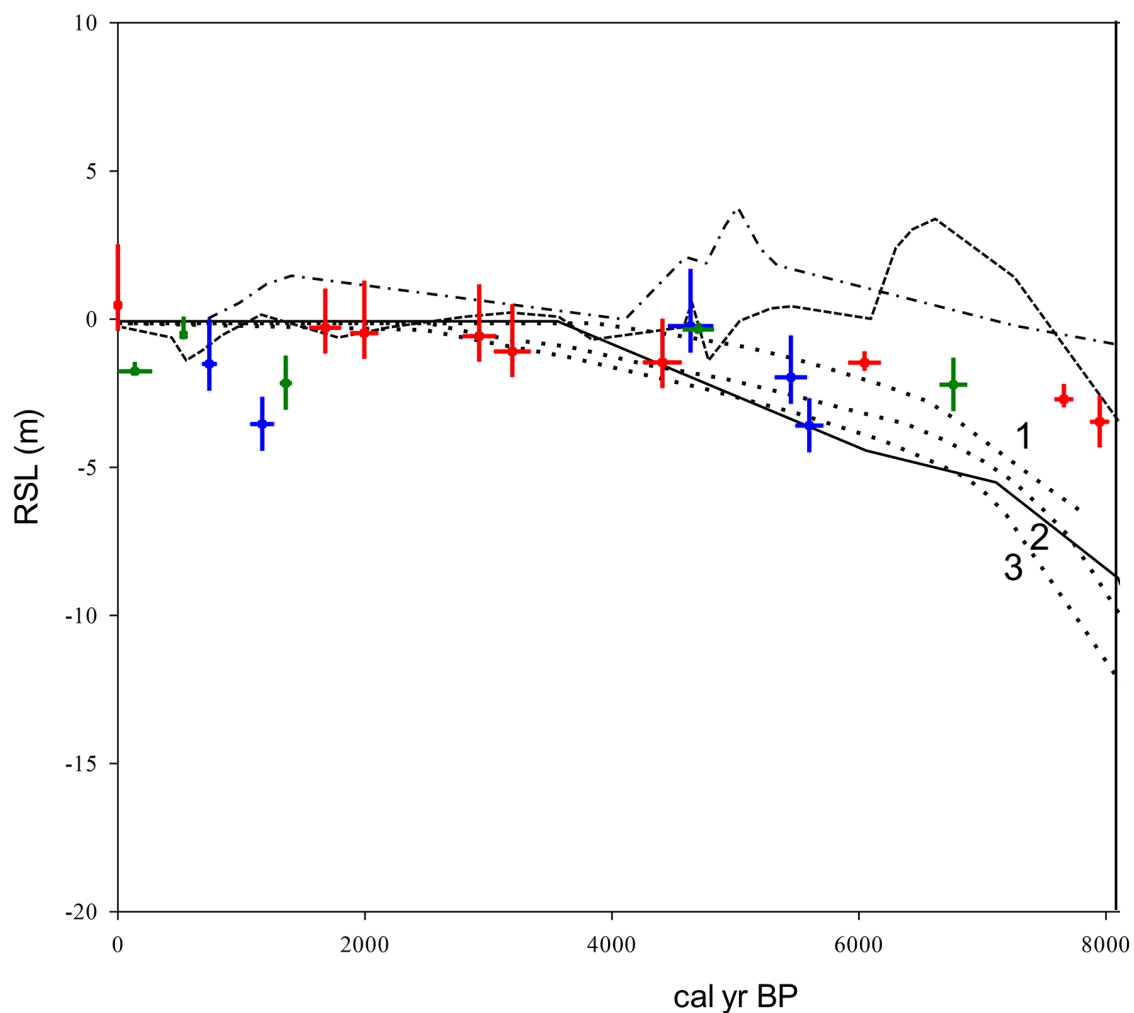
-○..... ANR
-▽..... BNR
-△..... CNR

Makoba Bay

- ▲--- AMAK-1
- BMAK-1
- ★--- CMAK-1

Unguja Ukuu

- A-UU-1
- ◇--- B-UU-1
- ◆--- C-UU-1
- ×--- C-UU-4



— RSL from The northern Rufiji Delta
— RSL from Makoba Bay
— RSL from Unguja Ukuu

- - - RSL from Compton (2001)
 - . - RSL from Ramsay and Cooper (2002)
 . . . RSL from Camoin et al. (1997; 2004)
 (1) Mauritius, (2) Mayotte, (3) Réunion
 — RSL from Zinke *et al.* (2003)